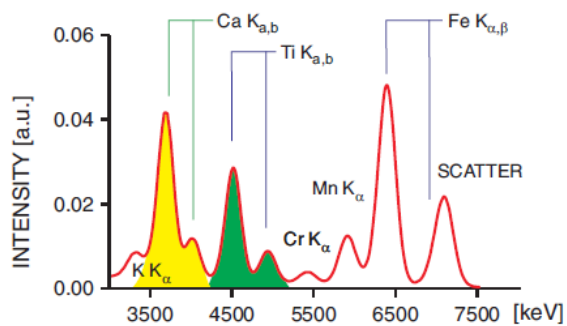
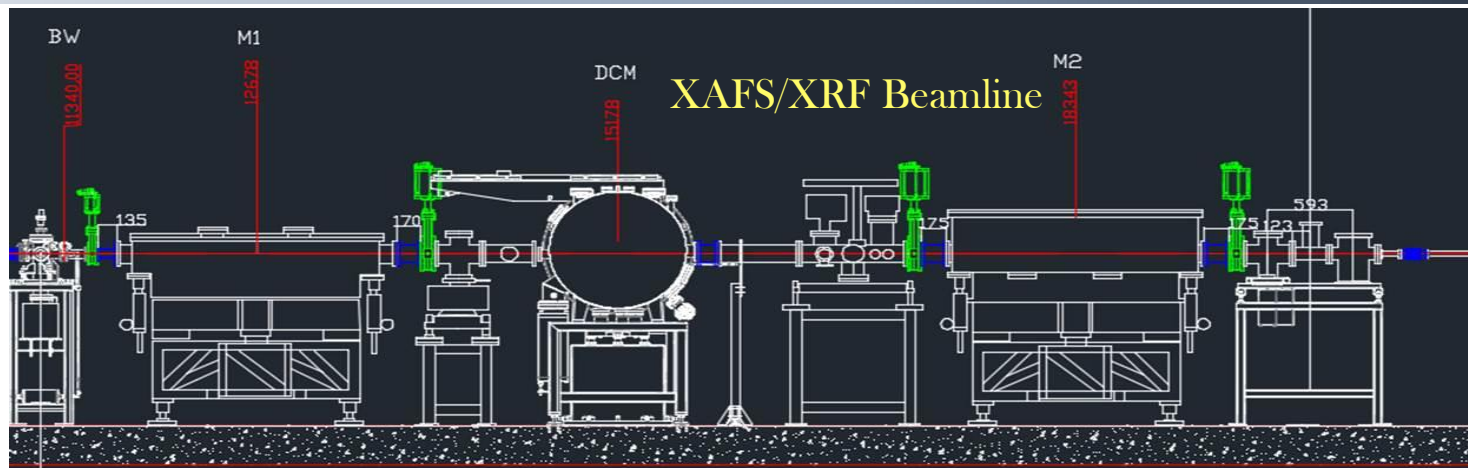


# X-ray Absorption/Emission and Optical Photons



SESAME

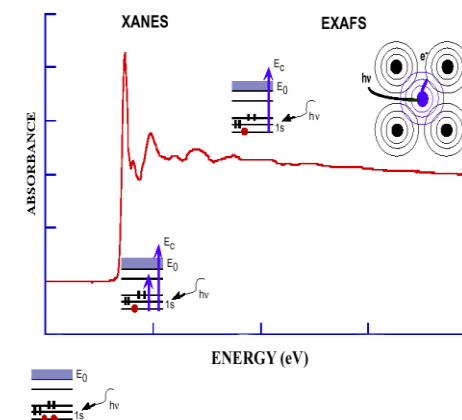


School on  
Synchrotron Light Sources  
and their Applications

23 January - 3 February 2023  
An ICTP online Meeting  
Trieste, Italy

ICTP

The Abdus Salam  
International Center  
for Theoretical Physics



Latif Ullah Khan

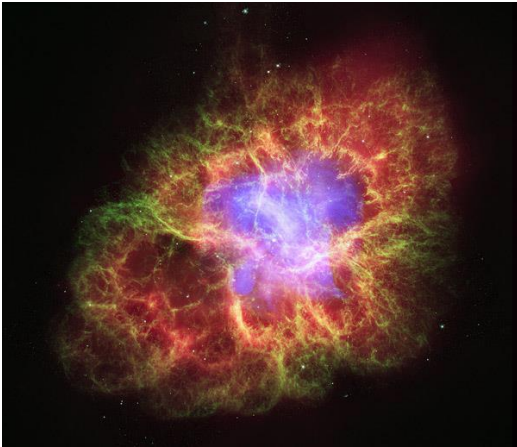
XAFS/XRF Beamline Scientist

Email: [latifullah.khan@sesame.org.jo](mailto:latifullah.khan@sesame.org.jo)

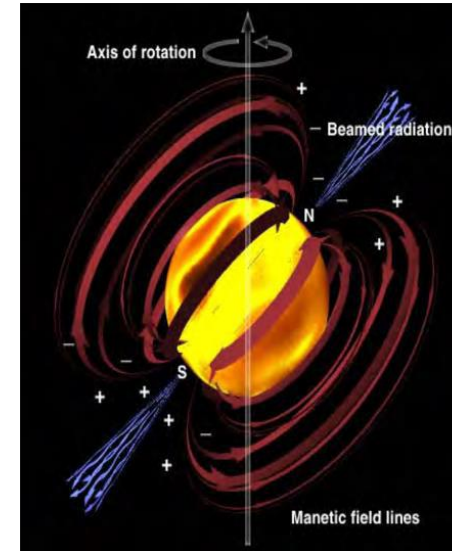
Date: January 26, 2023

# Natural Synchrotron Source

## *Crab Nebula*



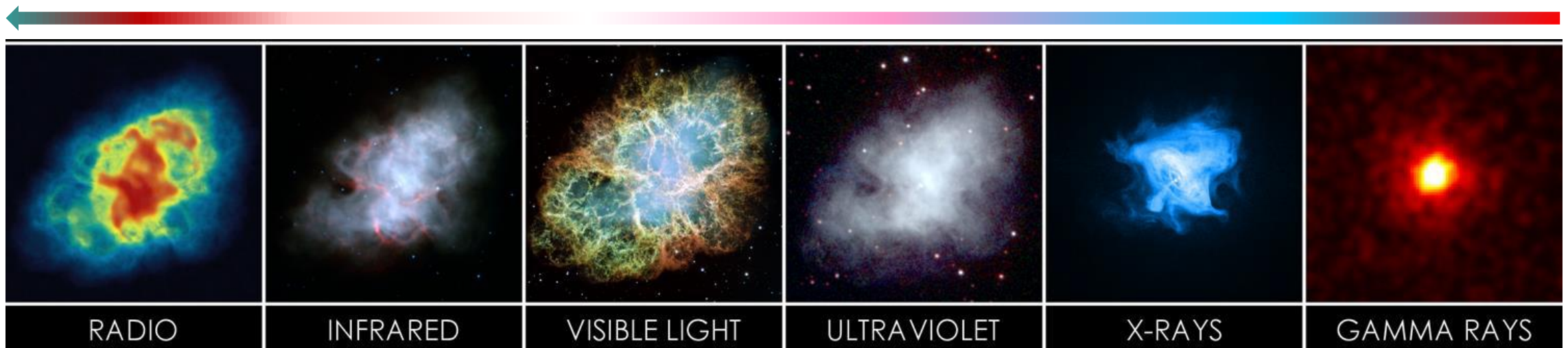
- ❑ **Crab pulsar** emits pulses of radiation from gamma rays to radio waves
- ❑ **Crab Nebula** is generally the brightest persistent gamma-ray source in the sky.



## *Crab pulsar*

- Neutron star
- 30 Km diameter
- 30 Hz rotation
- 108T magnetic field

## *Images at different frequencies*





# SESAME Synchrotron Light Source



SESAME Light Source

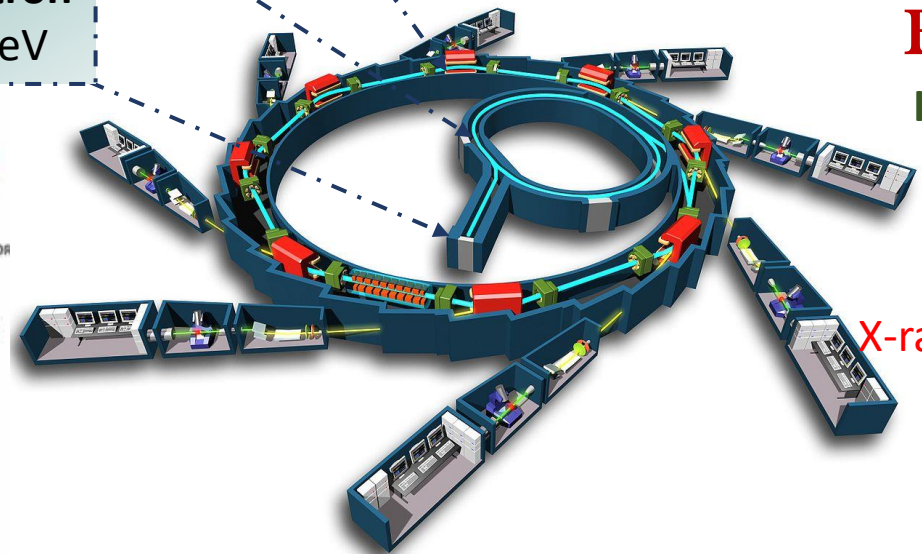
## SESAME Accelerator

- Circumference: 133.2 m
- Operation current: 300 mA
- Natural emittance: 26 nmrad

Storage Ring  
2.5 GeV

Booster  
800 MeV

Microtron  
22 MeV



## Beamlines

- IR
- XAFS/XRF
- XRD
- Soft X-ray
- X-ray Tomography

## World Maps Synchrotron Light Sources



☐ There are now more than 60 synchrotrons and FELs around the world

# XAFS/XRF Beamline Optics

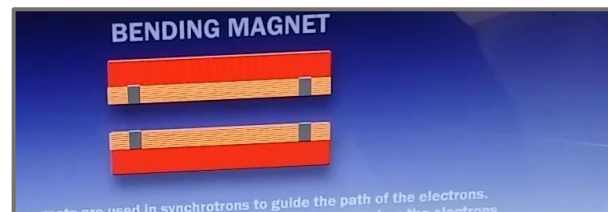
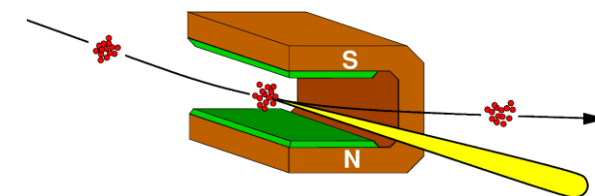


**VFM (M2)**  
(18328)

**DCM**  
(15178)

**CVD Window**  
**VCM (M1)** (11340)  
(12678)

**Source (D08)**  
**Bending Magnet**



Harfouche, M.; Abdellatif, Khan, L.U.; Paolucci, G. et al. Emergence of the first XAFS/XRF beamline in the Middle East: providing studies of elements and their atomic/electronic structure in pluridisciplinary research fields. *J. Synchrotron Rad.* 29, 1-7, 2022.



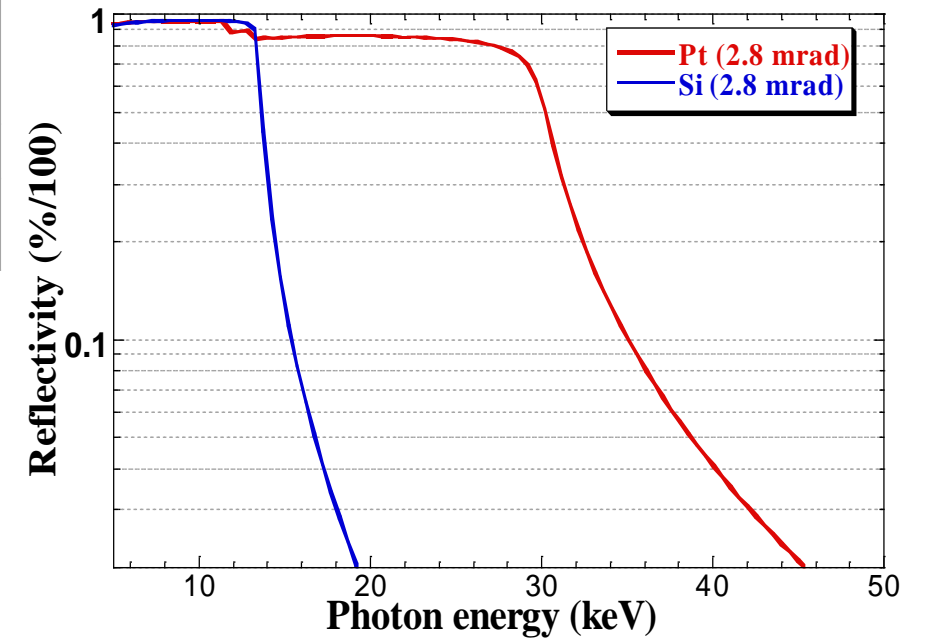
# Beamline Specifications



Parameter	Value
Magnetic field (BM)	1.4554 T
Energy Range	4.7 keV – 30 keV
Energy Resolution	
Si (111)	$10^{-4}$
Si (311)	
Flux	$5 \times 10^{11}$ Ph/s @ 8 keV
Beam size (Horizontal x Vertical)	determined by slits "H x V" (max: 20 x 5 mm <sup>2</sup> ) (min: 1 x 1 mm <sup>2</sup> )

## Specifications of the Collimating and Focusing Mirrors

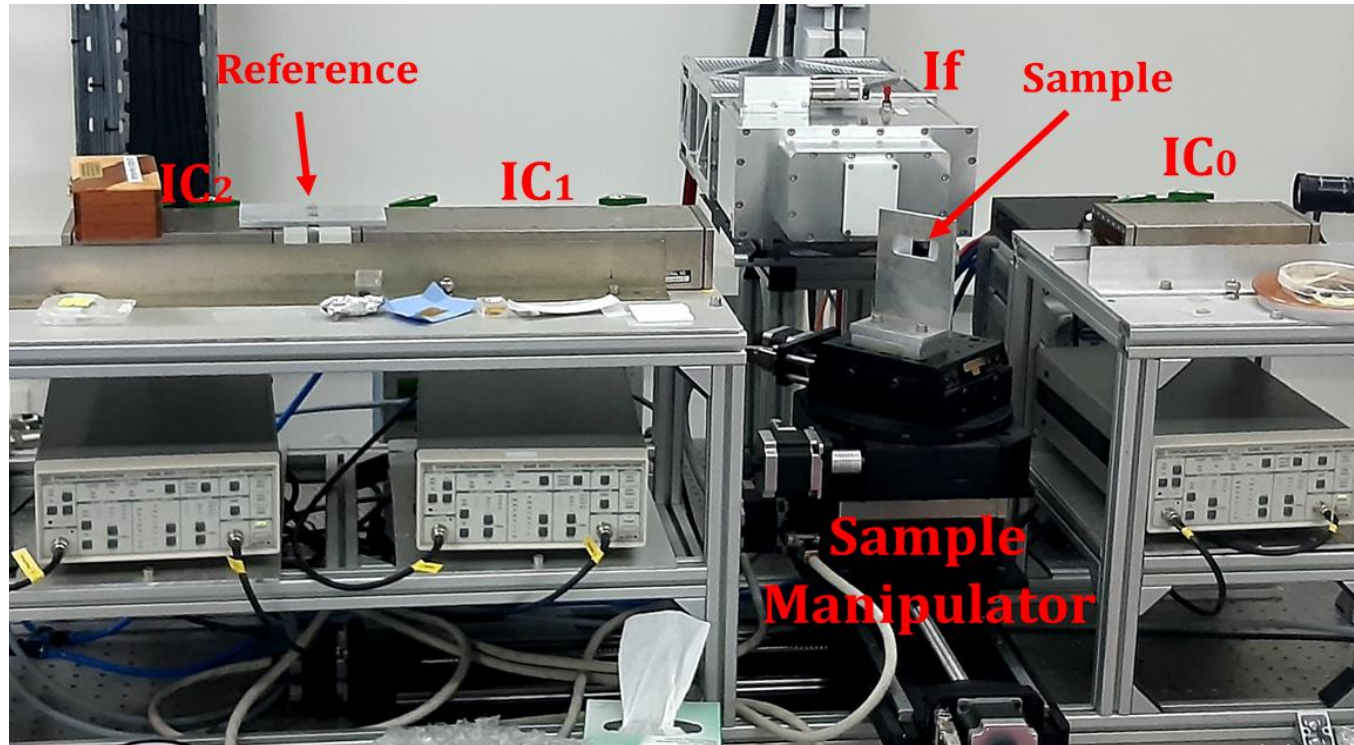
Specification	VCM (M1)	VFM (M2)
Dimensions (mm)	1200 x 70	1200x150
Coatings	Si, Pt	Si, Pt
Angle of incidence	Variable	Variable
Substrate	Silicon single crystal	ZERODUR
Cooling	Water cooled	Uncooled
Flatness	Cylindrical	Cylindrical
Type of bender	Pneumatic	Pneumatic
Minimum radius (km)	5.3	5.3



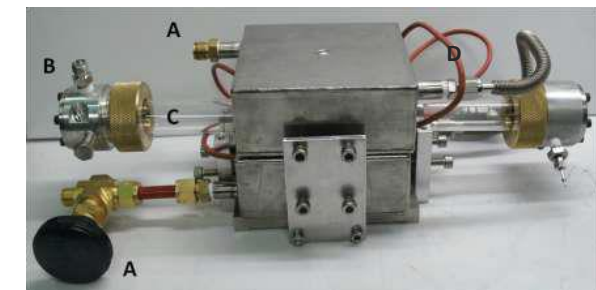
Mirrors reflectivity at 2.8 *mrad* incident beam angle for Pt and Si coatings

# End Station

## XAFS/XRF Experimental Station



Cryojet for cooling sample (~95 K)



Sample Environment - Tubular Furnace/Reactor (Prototype)

### Techniques available

- XAFS
- XRF
- XEOL (In Progress)

### XAFS measurement

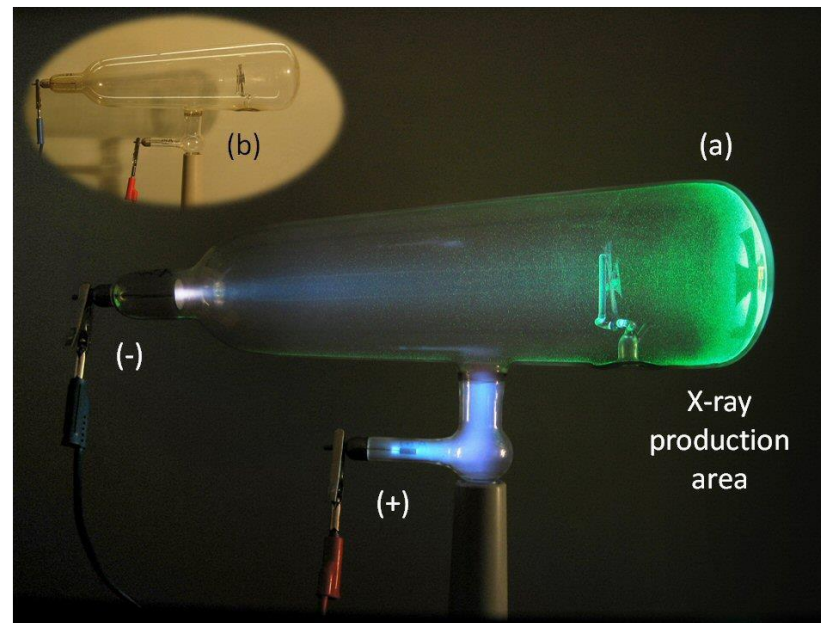
Transmission mode:  $\mu(E) = \log(I_0/I)$

Fluorescence mode:  $\mu(E) \propto I_f/I_0$

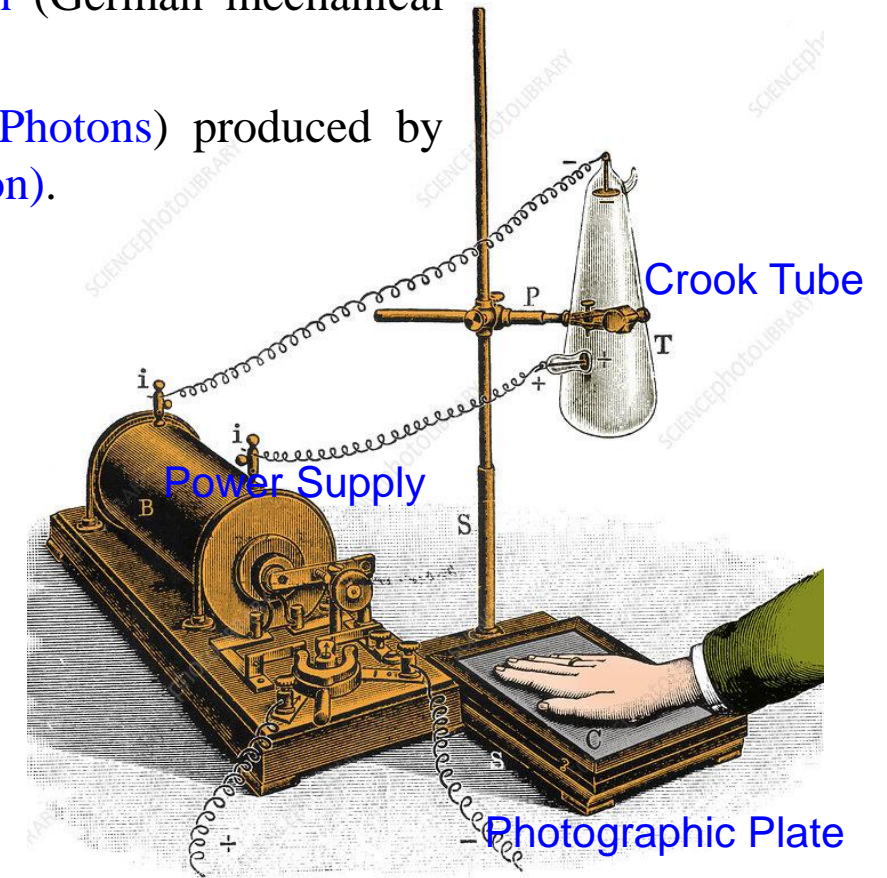


# X-ray Discovery and XAS/Luminescence

- X-ray absorption spectroscopy (XAS) adventure was started about one hundred years ago, after a while the discovery of X-rays in 1895 by **Wilhelm Conrad Röntgen** (German mechanical engineer and physicist).
- Röntgen discovered the X-ray from the LUMINESCENCE (Optical Photons) produced by screen of barium platinocyanide as a result of X-ray Absorption (Excitation).



**Wilhelm Röntgen** discovered X-rays using the Crookes tube.



**Drawing of the X-ray machine** used by Wilhelm Roentgen to produce images of the hand.

# First X-ray Absorption Spectrum

- The first X-ray absorption spectrum was observed by de Broglie in 1913, after a while the discovery of X-rays by Röntgen (1895). In his X-ray absorption experiment, de Broglie used X-ray tube as a source and mounted a single crystal on the cylinder of a recording barometer, employing a clockwork mechanism to rotate the crystal around its vertical axis at a constant angular speed. As the crystal was rotated, the X-rays scattered at all angles between the incident beam and the diffraction planes, according to the Bragg law, and consequently change the X-ray energy  $E$ :

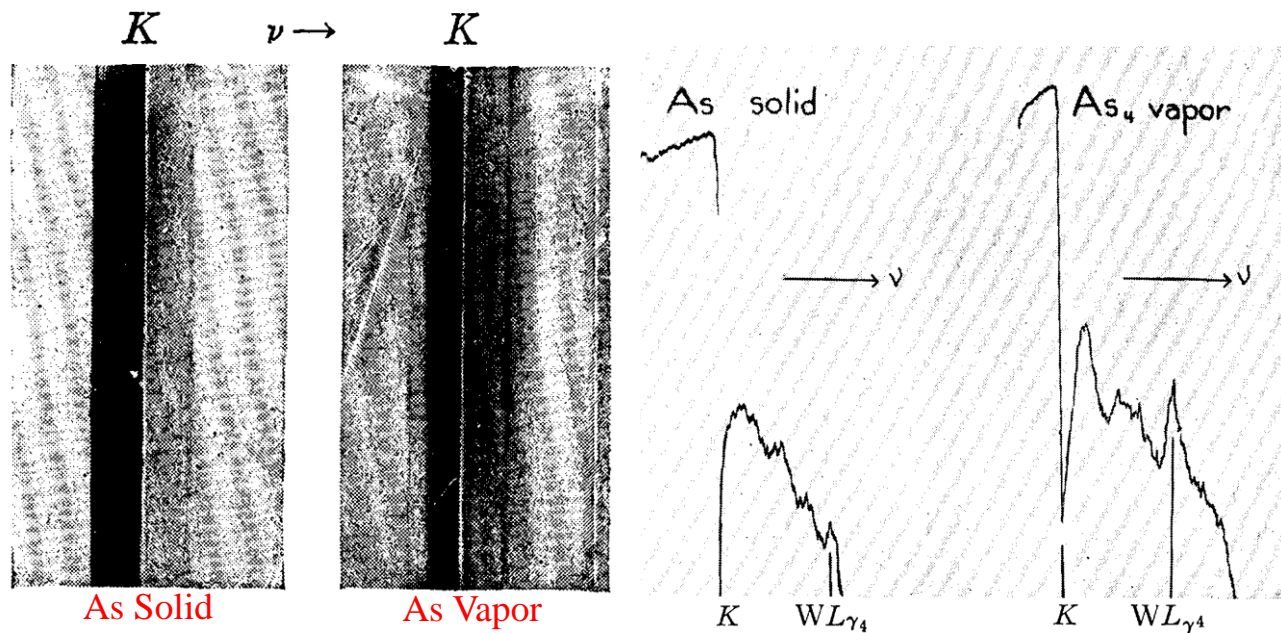
$$2d_{hkl} \sin \theta = \lambda = hc/E$$

$c$ : Speed of light ( $c = 2.9979 \cdot 10^8$  m/s)

$h$ : Planck constant ( $h = 6.626 \times 10^{-34}$  J s)

Thus,  $hc = 12.3984 \text{ \AA keV}$

- He recorded the X-rays of varying intensities on a photographic plate and observed two distinct discontinuities on the film, proving to be the K-edge absorption spectra of silver and bromine atoms present in photographic emulsion.
- This experiment provided a foundation for the modern monochromatic beam (Monochromator)



J. D. Hanawalt, The Dependence of X-ray Absorption Spectra upon Chemical and Physical State. *Phys. Rev.* 1931, 37, 715.



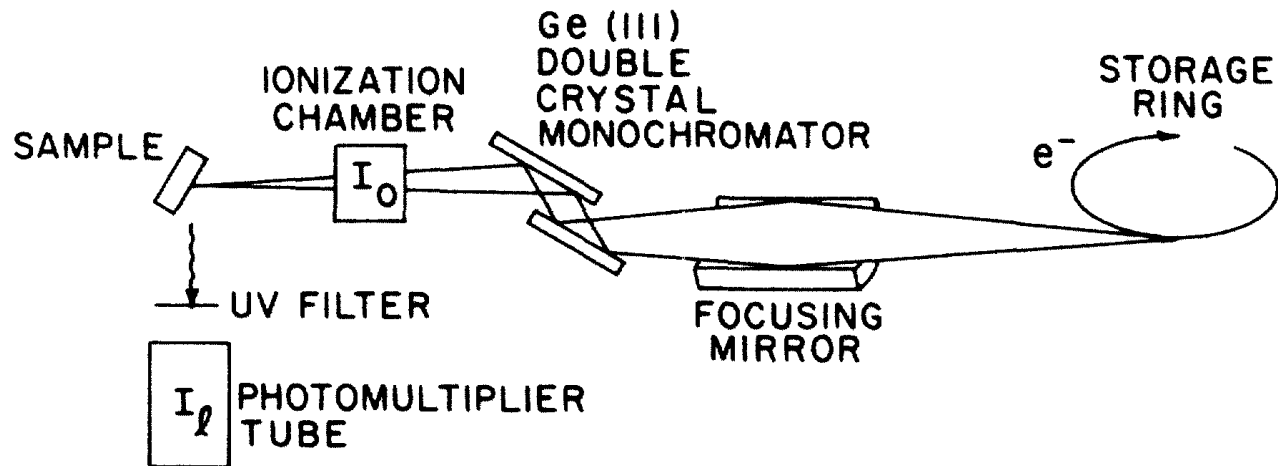
# XEOL



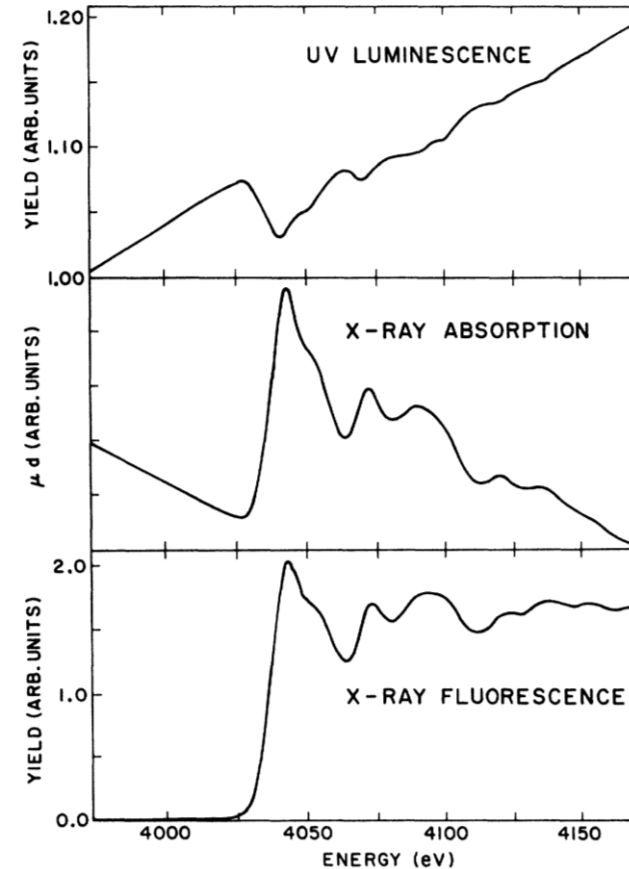
- ❑ A crucial relation between the X-ray photon and optical photon is manifested by **X-ray Excited Optical Luminescence (XEOL)**.
- ❑ **XEOL** demonstrates the fundamental mechanism of the conversion of X-ray energy absorbed by the system to optical photons.
- ❑ XEOL was successfully exploited over the past decades for a quantitative detection of rare earth ions at the ultra-trace level (part per billion) in high purity inorganic hosts.
- ❑ **XEOL** is often used together with XANES/NEXAFS to provide site specificity and reveal the electronic structure and optical properties of the wide range of materials, such as rare earth phosphors, semiconductors, quantum dots etc., applying in display/lighting technologies (e.g., LED lamps, TV, smartphone screen etc.), scintillators (X-ray/Gamma rays detectors) and energy conversion devices (Photovoltaic cells).
- ❑ Now a days mostly synchrotron light sources have **XEOL** facility (Applications: **XEOL** Spectra, XAFS in **XEOL** mode, **XEOL** imaging or element selective mapping of heterogeneous materials with submicron resolution).

# First XAFS in XEOL Mode

- First XAFS in X-ray excited optical luminescence (XEOL) mode by [Antonio Bianconi](#) at Stanford Synchrotron Radiation Project 1978



Experimental Setup



XAFS in XEOL mode

XAFS in Transmission mode

XAFS in Fluorescence mode

Ca K-edge XAFS of  $\text{CaF}_2$




# Rare Earths

H																	He														
Li	Be											B	C	N	O	F	Ne														
Na	Mg											Al	Si	P	S	Cl	Ar														
K	Ca	Sc											Ti	V	Cr	Mn	Fe	Co	Ni	Cu	Zn	Ga	Ge	As	Se	Br	Kr				
Rb	Sr	Y											Zr	Nb	Mo	Tc	Ru	Rh	Pd	Ag	Cd	In	Sn	Sb	Te	I	Xe				
Cs	Ba	La	Ce	Pr	Nd	Pm	Sm	Eu	Gd	Tb	Dy	Ho	Er	Tm	Yb	Lu	Hf	Ta	W	Re	Os	Ir	Pt	Au	Hg	Tl	Pb	Bi	Po	At	Rn
Fr	Ra	Ac	Th	Pa	U	Np	Pu	Am	Cm	Bk	Cf	Es	Fm	Md	No	Lr	Rf	Db	Sg	Bh	Hs	Mt									

Sc <sup>3+</sup>																
Y <sup>3+</sup>																
	Ce <sup>4+</sup>	Pr <sup>4+</sup>											Tb <sup>4+</sup>			
La <sup>3+</sup>	Ce <sup>3+</sup>	Pr <sup>3+</sup>	Nd <sup>3+</sup>	Pm <sup>3+</sup>	Sm <sup>3+</sup>	Eu <sup>3+</sup>	Gd <sup>3+</sup>	Tb <sup>3+</sup>	Dy <sup>3+</sup>	Ho <sup>3+</sup>	Er <sup>3+</sup>	Tm <sup>3+</sup>	Yb <sup>3+</sup>	Lu <sup>3+</sup>		
					Sm <sup>2+</sup>	Eu <sup>2+</sup>						Tm <sup>2+</sup>	Yb <sup>2+</sup>			

Tm – least abundant of the RE (0.5 ppm)  It is more abundant than Cd, Ag, Pt, Au, Se...

# Rare Earths Applications

## Applications of Phosphors

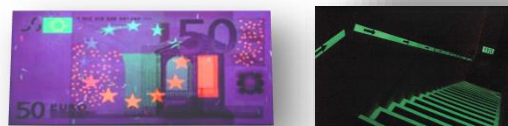
### Lighting and Display

97% volume (9500T)



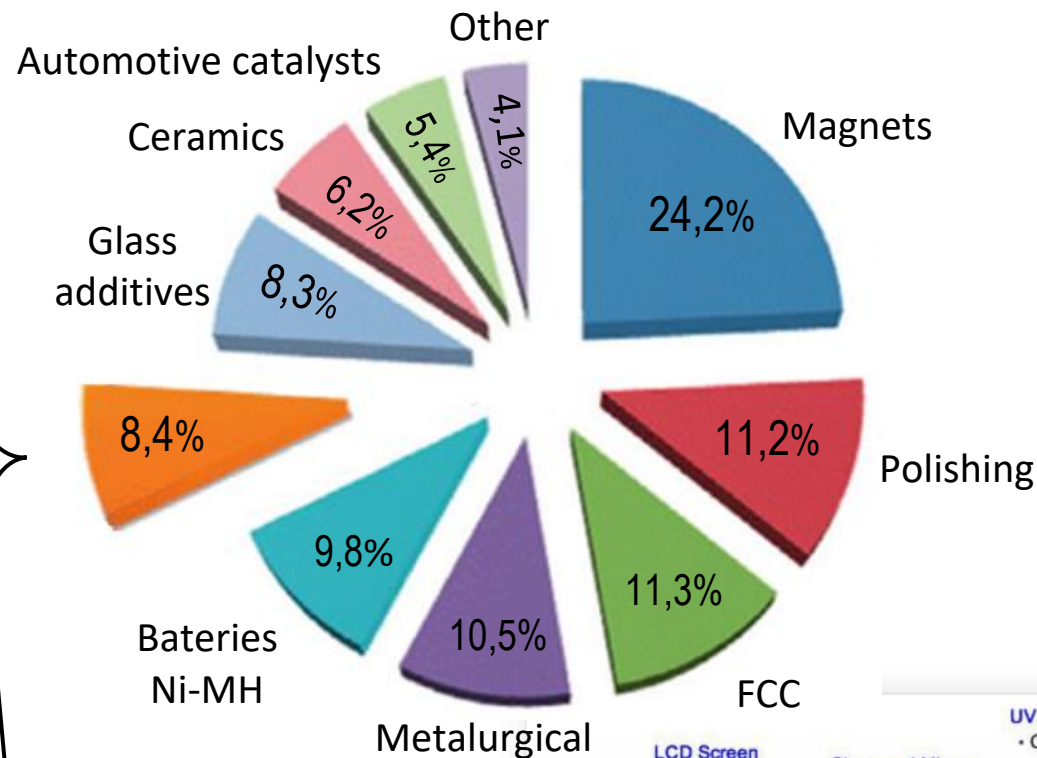
Y 69,6%	Ce 10,9%	La 8,3%
Eu 4,9%	Tb 4,5%	Gd 1,8%

### Medical (Other) Laser and Scintillator



Optical Markers

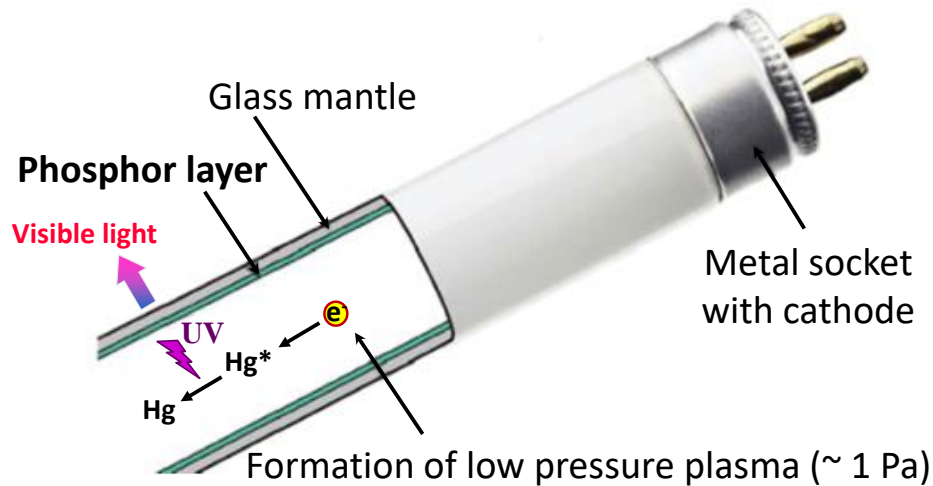
Persistent luminescent





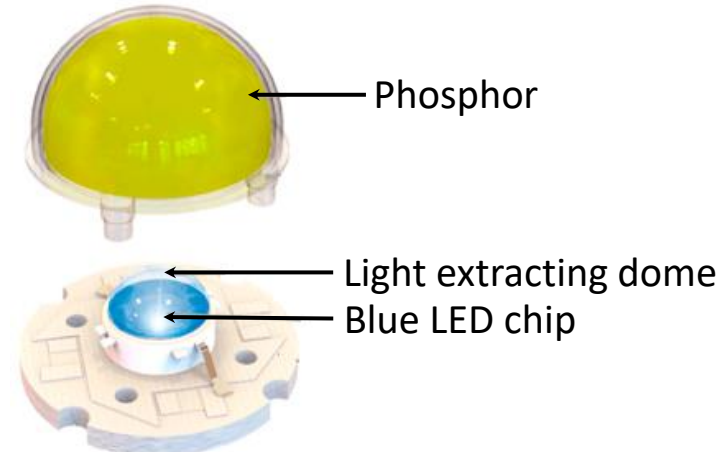
# Evolution of Lighting Technology

## How fluorescent lamp work?



Phosphor		Emission
$Y_2O_3:Eu^{3+}$	(YOE)	Red
$(Ce^{3+},Tb^{3+})MgAl_{11}O_{19}$	(CAT)	Green
$BaMgAl_{10}O_{17}:Eu^{2+}$	(BAM)	Blue

## White LED lamp



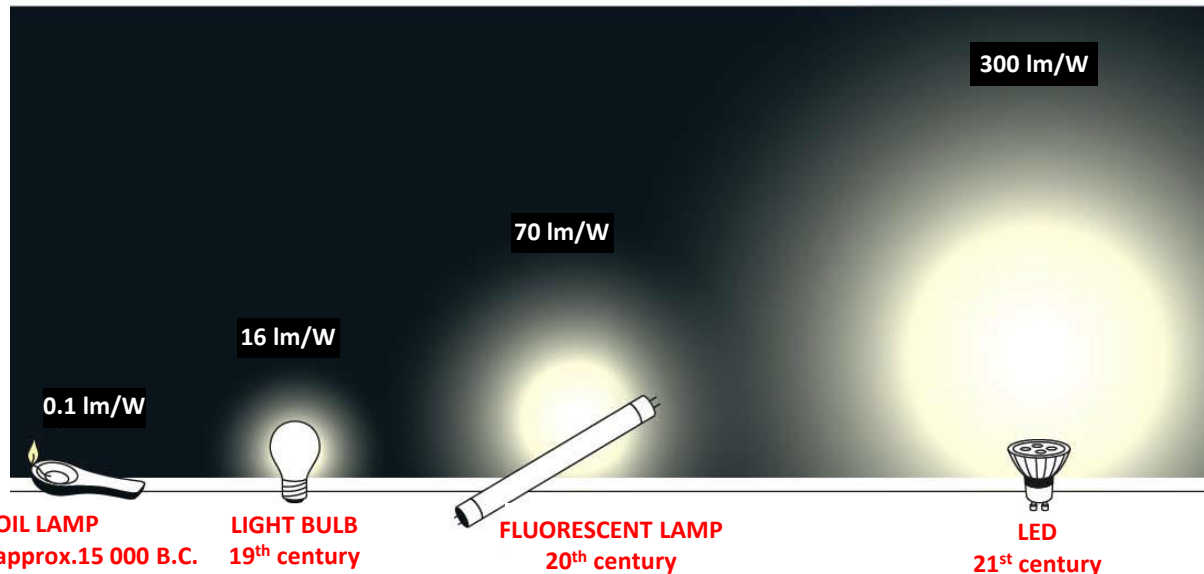
**Phosphor:**  $Y_3Al_5O_{12}:Ce^{3+}$  (YAG:Ce)  
**Emission color:** Yellow



## Energy Savings Impact

- ~ 40 % Electricity Savings (261 TWh) in USA in 2030 due to LEDs
- Eliminates the need for 30+ 1000 MW Power Plants by 2030
- Avoids Generating ~ 185 million tons of CO<sub>2</sub>

(SHUJI NAKAMURA Nobel Prize 2014)



# Global Rare Earths Mines Reserves

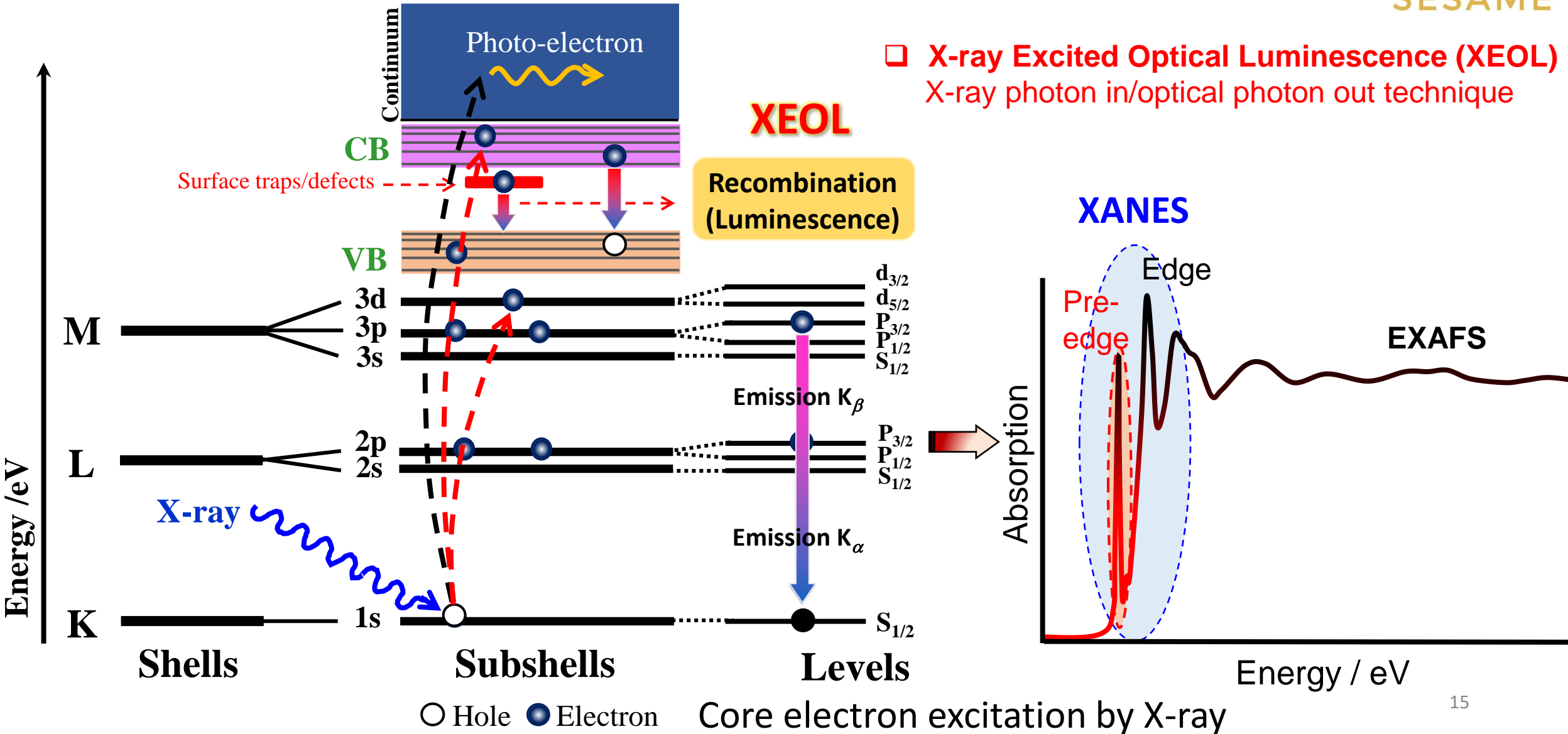


- **World total reserves (rounded about): 120,000,000 tons (120 million metric tons)**
- **China: 44,000,000 tons or 44 million metric tons (36%)**



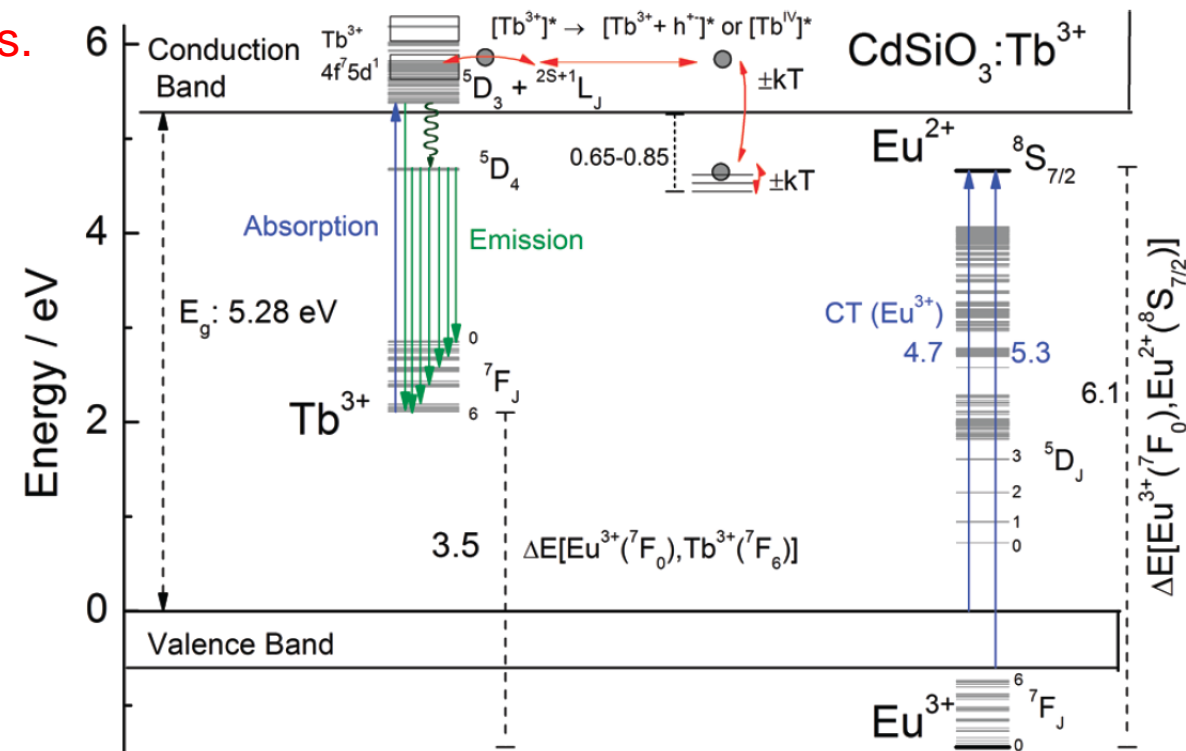


# X-ray Absorption and Electron Excitation Mechanism



# Persistent Luminescence Mechanism

- For full understanding of luminescence in a **solid state materials (phosphors)**, the energy level structures need to be studied for:
  - The host.
  - The luminescent ions. (Emission center)
  - Structural defects.

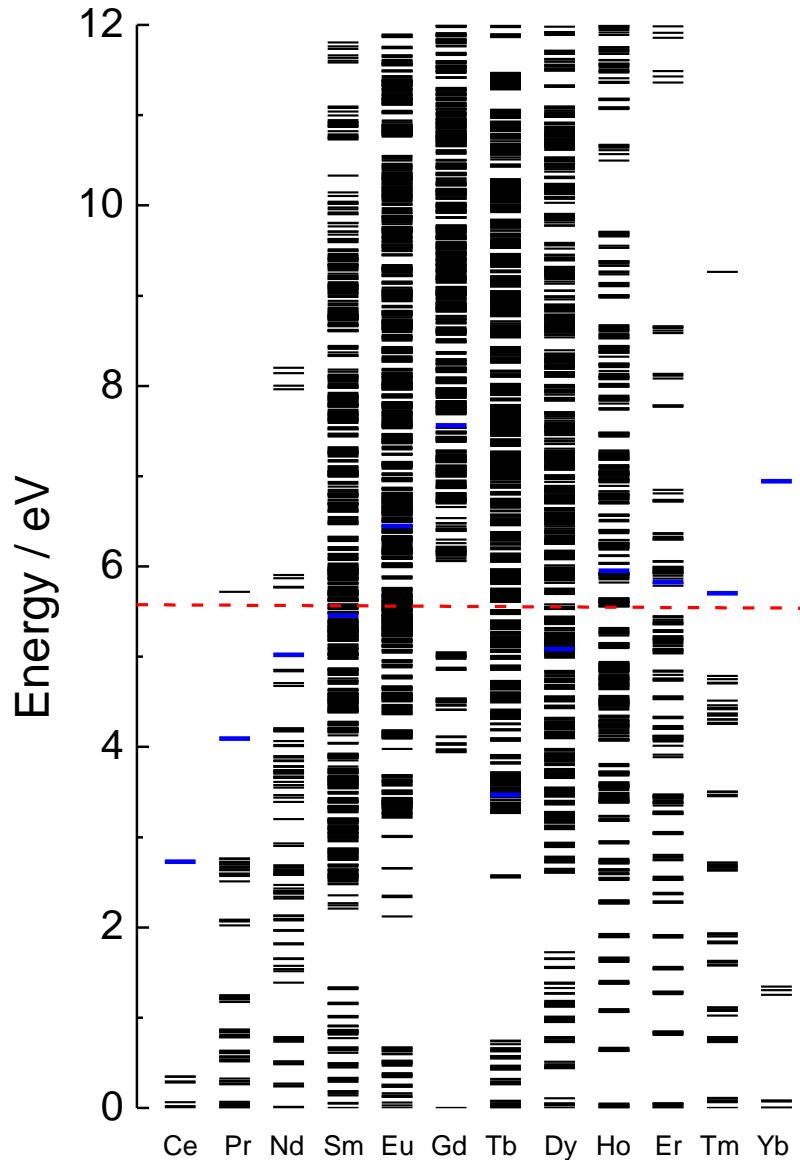


Persistent luminescence mechanism of  $\text{Tb}^{3+}$  in  $\text{CdSiO}_3$ .

- Goal: models for predicting the luminescence properties of materials.
  - Combining experimental (optical) and theoretical methods.
  - Probing metal ions (emission center) by X-ray absorption.



# Lanthanides (Ln<sup>3+</sup>) Energy Levels: 4-10 eV Energy Range



Energy levels structure of trivalent lanthanides ions.

## Energy range 4-10 eV needed for:

- Host band gap energy ( $E_g$ ) determination.
  - Essential for e.g. persistent luminescence materials.
    - Example: 7.1 eV for  $\text{Sr}_2\text{MgSi}_2\text{O}_7:\text{Eu}^{2+},\text{Dy}^{3+}$ .
- Study of dopant energy levels structure in the VUV range ( $> 6$  eV).
  - High 4f levels and 5d levels.
    - Quantum cutting materials (e.g.  $\text{KMgF}_3:\text{Pr}^{3+}$ ).
- Higher photon flux needed than with lab equipment.
  - High sensitivity.
- Measuring fast kinetics (ns) and time resolution.
- Synchrotron light sources offer a better temporal stability in terms of the duration, amplitude and repetition rate of the pulses than the most sophisticated pulsed lasers.

High energy limit of laboratory set-ups: 5.6 eV.

# RE<sup>3+</sup> β-Diketonates

## □ Sm<sup>3+</sup>, Gd<sup>3+</sup> and Eu<sup>3+</sup> β-diketonates

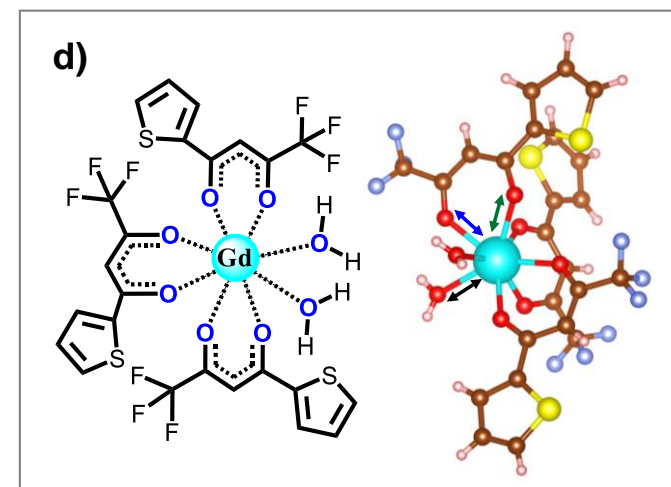
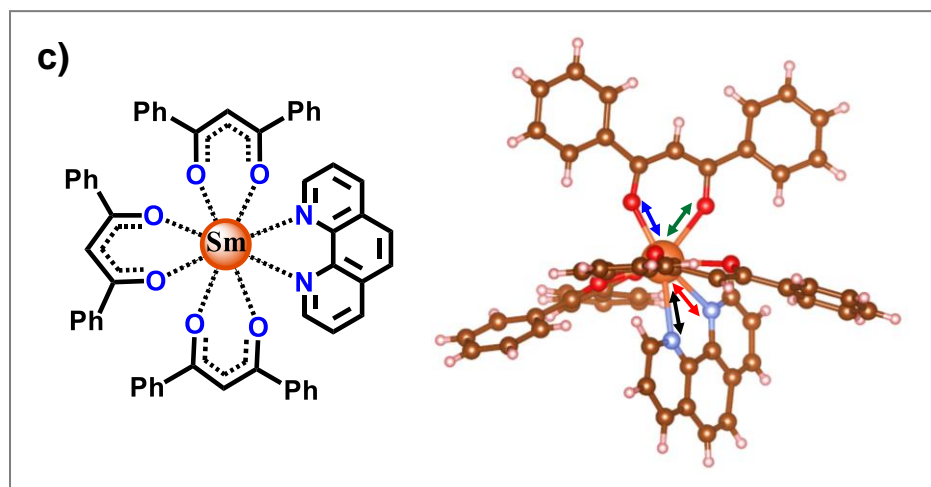
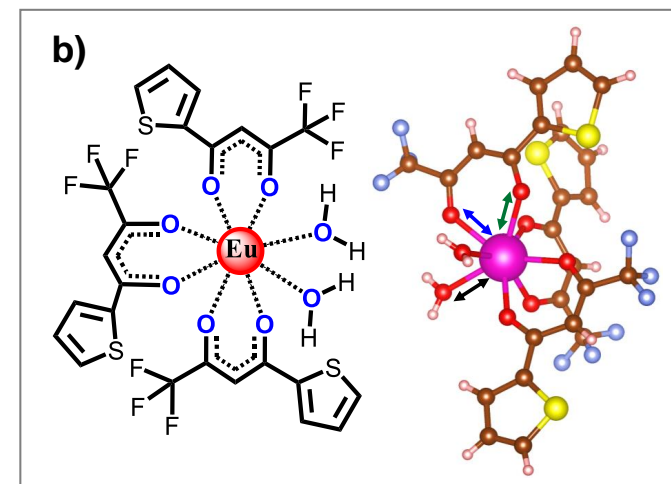
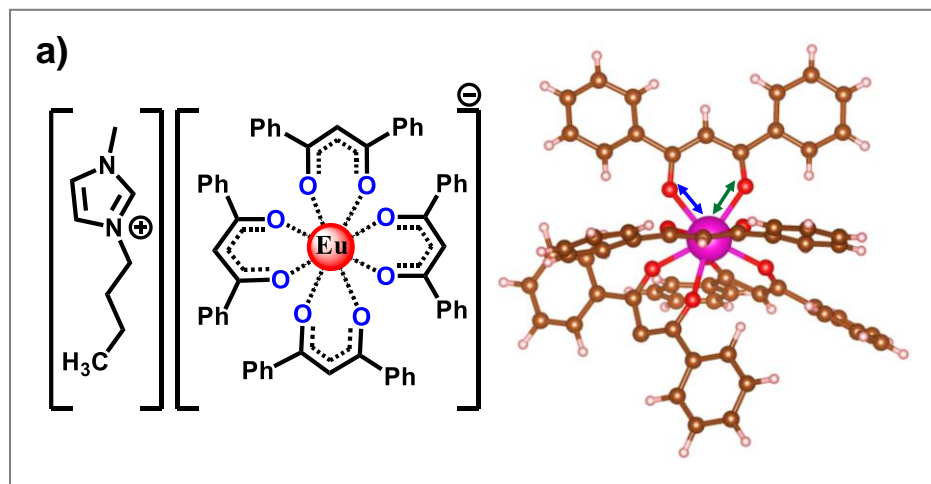
□ Fabrication of single-layer organic light-emitting memory devices

□ Modern optical quantum memories

□ Organic light emitting diodes (OLEDs).

□ Gd (III) complex, an excellent T<sub>1</sub> contrast agents in MRI imaging

Samples provided by Prof. Hermi F. Brito, Laboratory of *f*-block elements, Institute of Chemistry University of Sao Paulo Brazil.

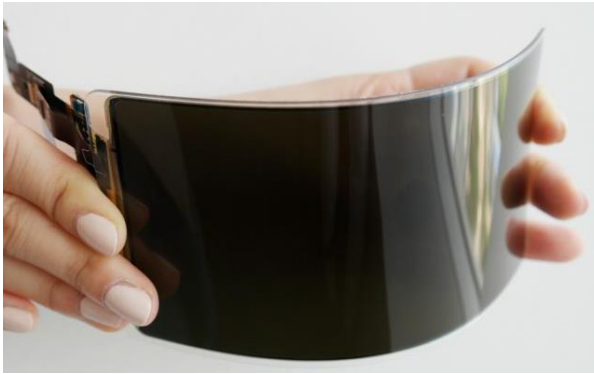


Khan, L. U. et al. A Strategy to Probe the Local Atomic Structure of Luminescent Rare Earth Complexes by XANES Simulation Using Machine Learning Based PyFitIt Approach. *Inorganic Chemistry (ACS)*, 2023 (Accepted - In Press ).



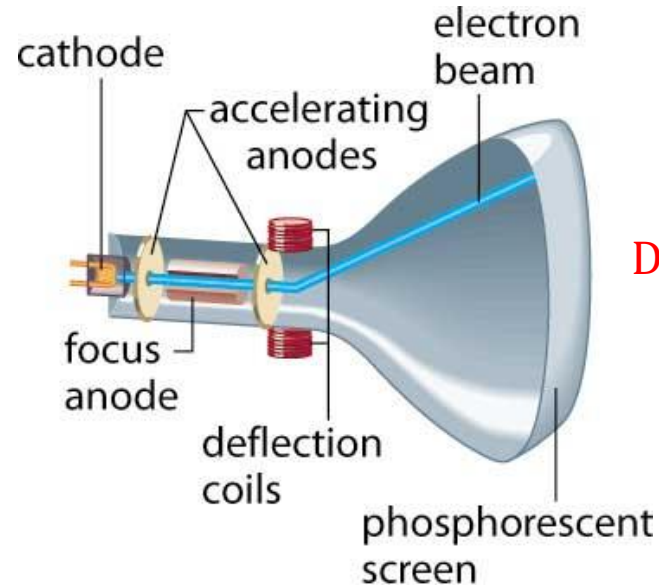
# Phosphors in Display Technologies

## Unbreakable OLED Display



Samsung

## Rare Earth Phosphors in TV Display



(Phosphors)

Development

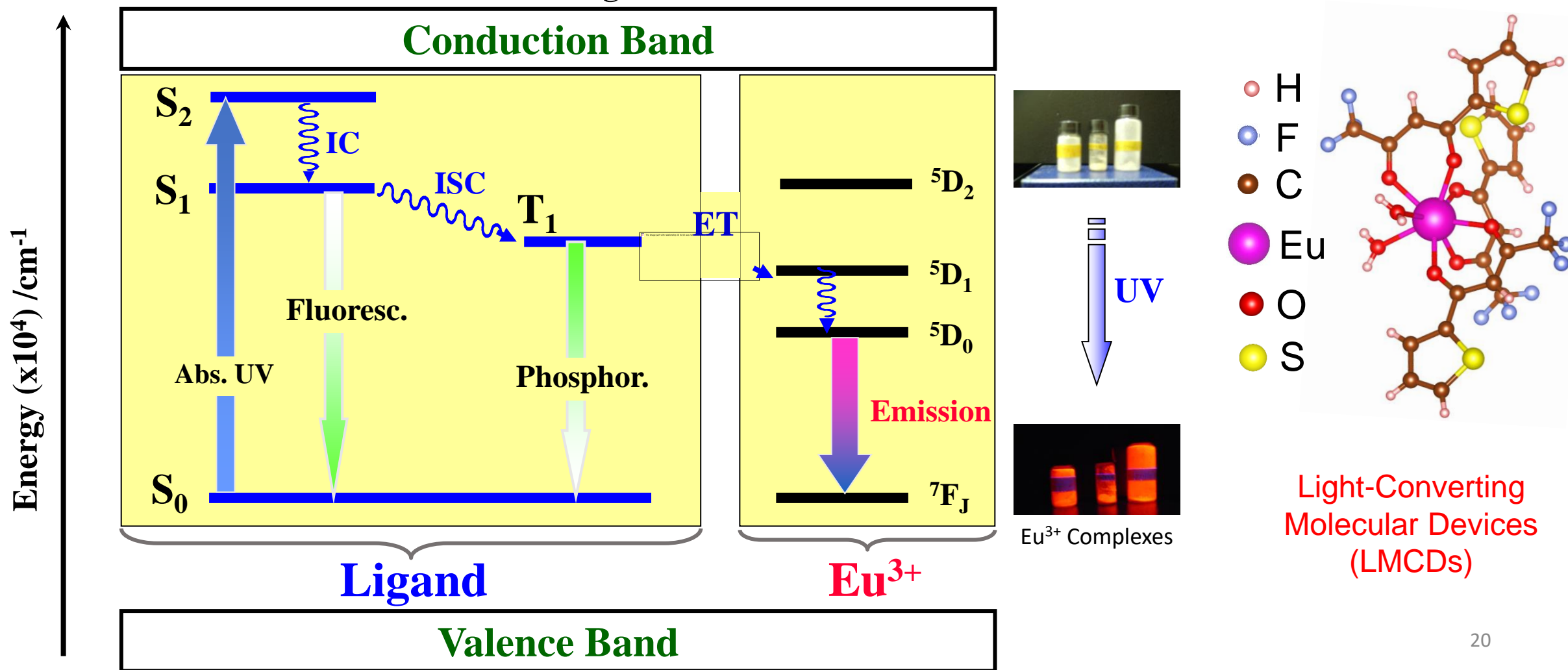


## OLED Display

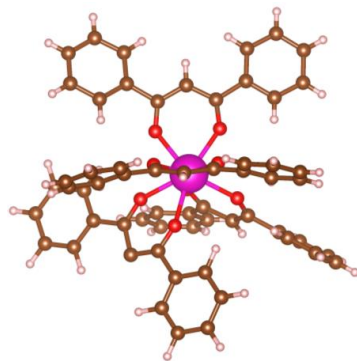
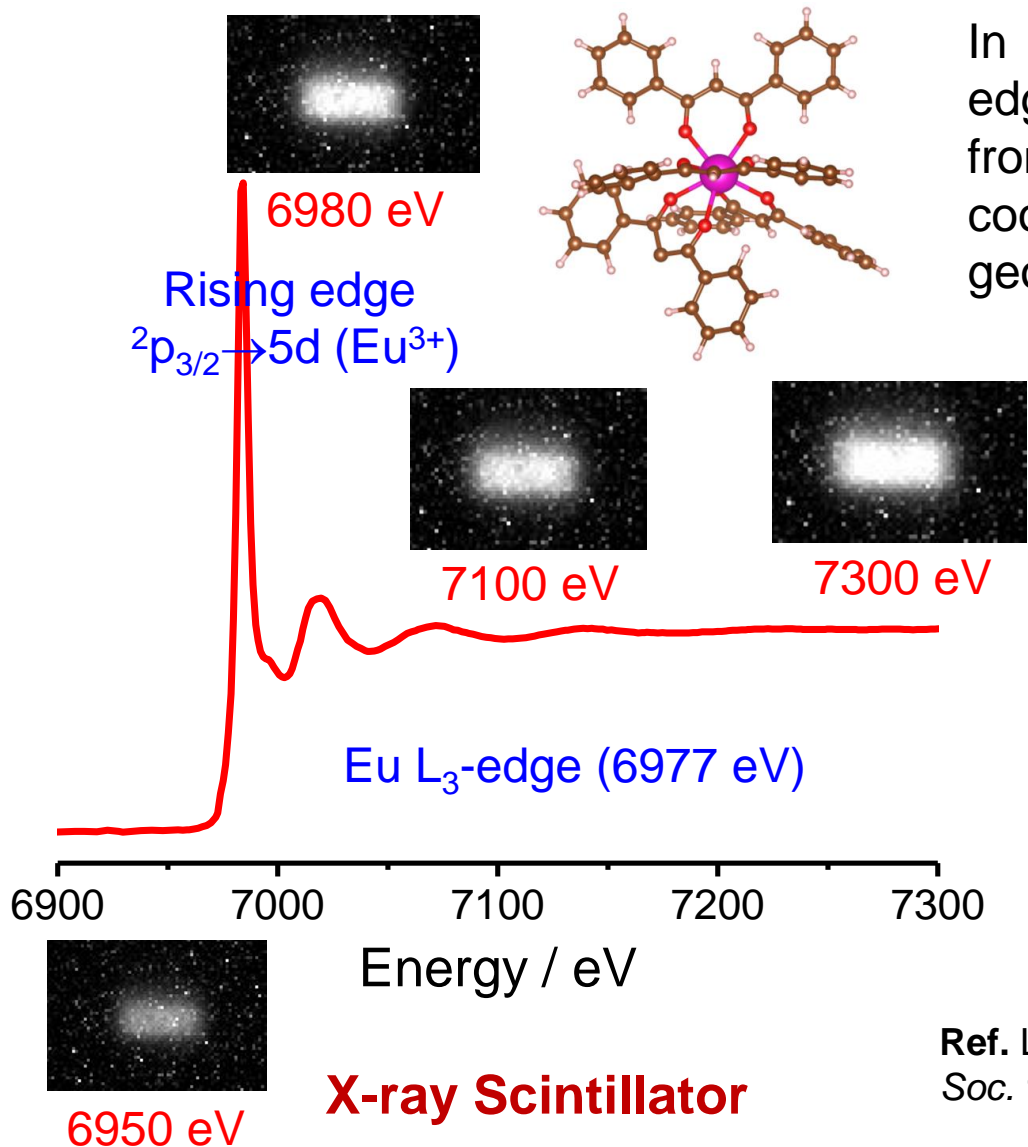


# Intramolecular Energy Transfer

Efficient: Absorption (L) → Transfer of energy Ligand-Eu<sup>3+</sup> → Emission (Eu)



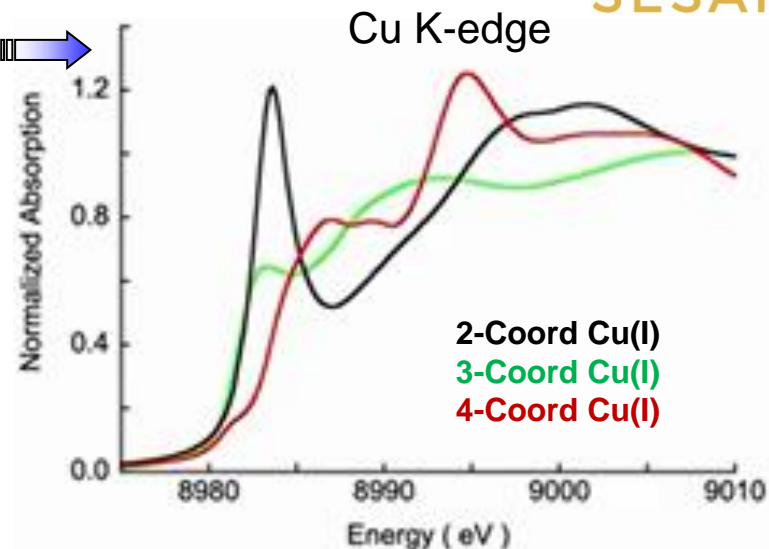
# Eu<sup>3+</sup> Complex: X-ray Scintillator (Optical Photons)



In d-transition metals, rising edge has strong contribution from  $1s \rightarrow 4p$ , dependent on coordination number and geometry (ligand field effect).

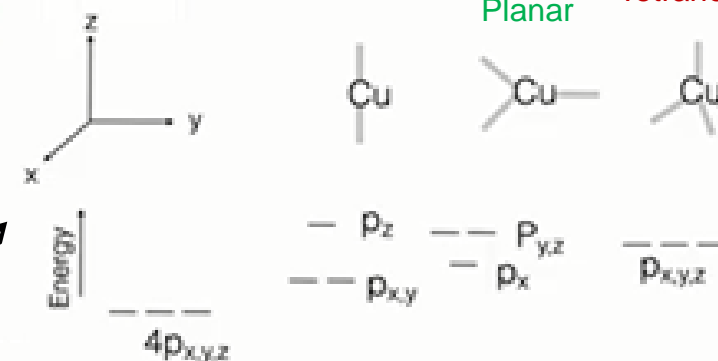
## Ligand field effect

Conf.	Ligand field (cm <sup>-1</sup> )
3d <sup>N</sup>	15000
4d <sup>N</sup>	20000
5d <sup>N</sup>	25000
4f <sup>N</sup>	300
5f <sup>N</sup>	2000



Coordination No:

2 Linear      3 Trigonal Planar      4 Tetrahedral

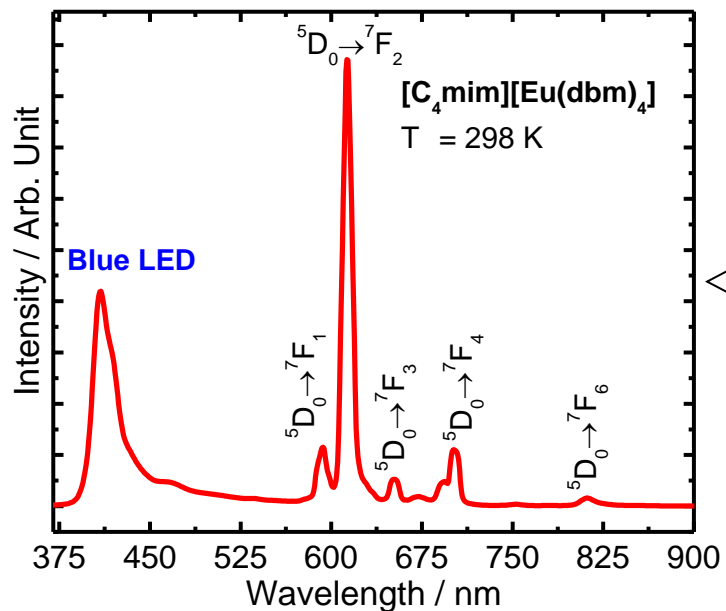


Ligand field splitting of copper 4p orbitals as a function of site geometry.

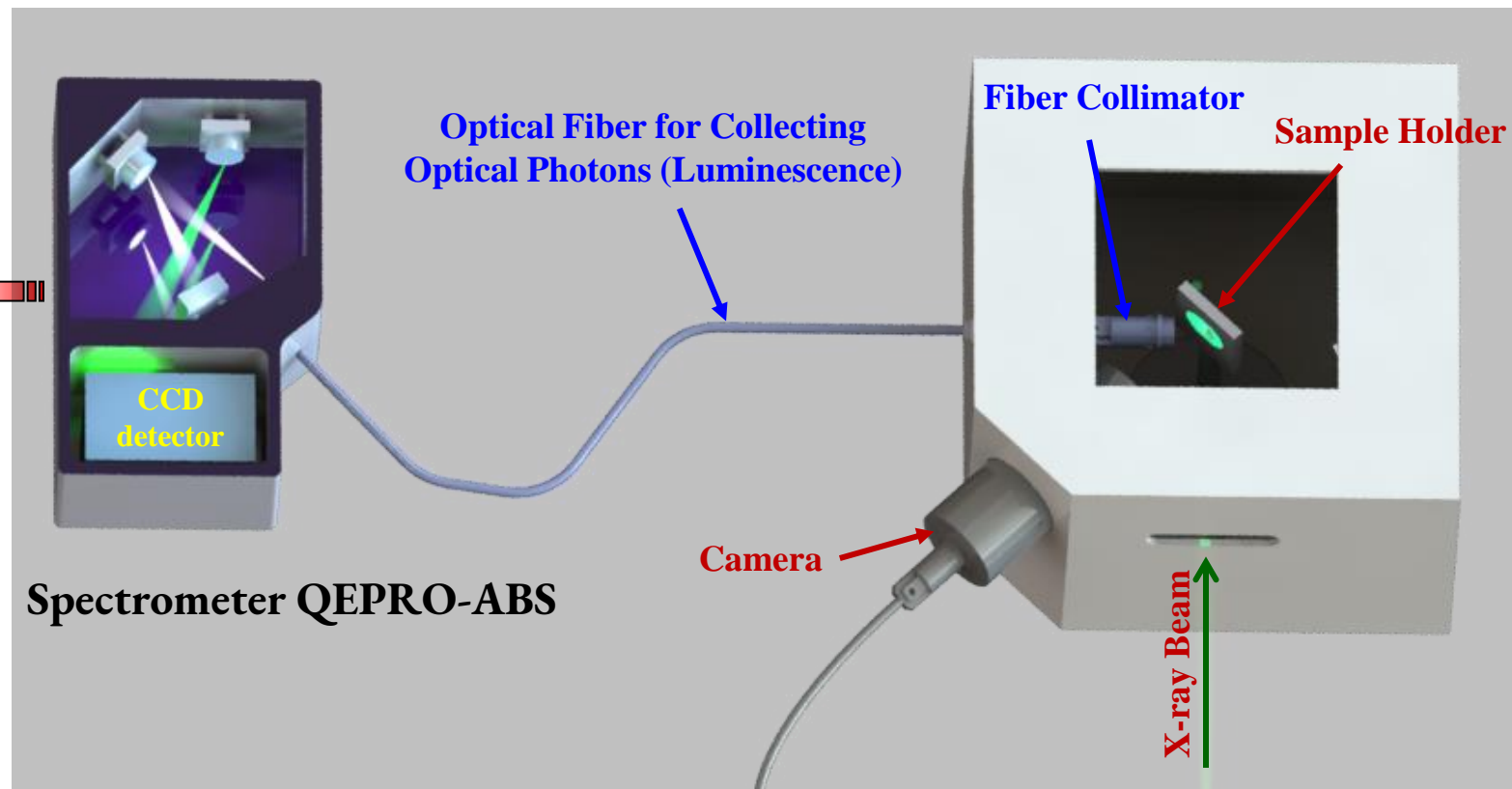
Ref. Lung-Shan Kau et al. *J. Am. Chem. Soc.* 1987, 109, 6433-6442.



# XEOL Setup



Emission Spectrum of Eu<sup>3+</sup> complex  
Measured with QEPRO-ABS (Exc. LEDs)



Abid Ur Rehman Mechanical Engineer

- X-ray Excited Optical Luminescence (XEOL) Spectroscopy
- Luminescence ( $\lambda$ : 200 - 920nm)
- XANES in XEOL mode











Project Grant from IAEA

# Machine Learning: XANES Simulation



- ❑ The modern data science-based machine learning is very attractive among the XAFS community to explore the X-ray absorption spectroscopy data of metals across the science.
- ❑ The quantitative structural determination from the XANES is largely demanded in catalysis, energy storage materials and metal complexes (XANES simulation by machine learning PyFitIt package).

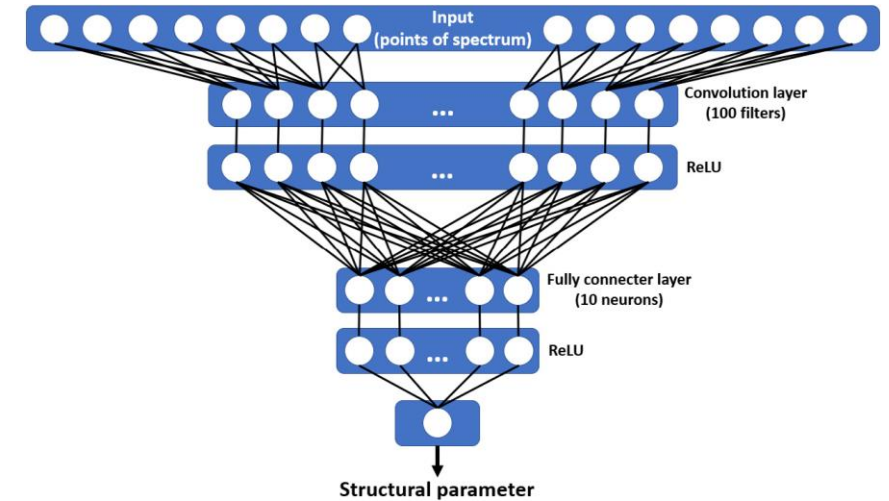
## Machine Learning: PyFitIt Inverse method

-  **00 Fitting Smooth**  Input data: Crystal structure (XYZ), experimental XANES and define FDMNES convolution parameters
-  **10 Create a project**  Photoabsorber selection, define geometry deformation within allowed limit (degrees of freedom) and FDMNES parameters for *ab-initio* XANES calculation
-  **20 Calculate XANES for a set of geometries**  Train a model on input data (100 samples), parallel calculations of theoretical XANES, needs multicores clusters [SESAME server 24 cores (CPUs)]
-  **30 Inverse approach**  Calculated spectrum from the step 20 and employ Euclidean ( $L_2$ ) norm, integral of the squared difference between the theoretical & experimental XANES spectrum
-  **50 Fitting XANES by sliders**  Fit by sliders within allowed limit of deformation

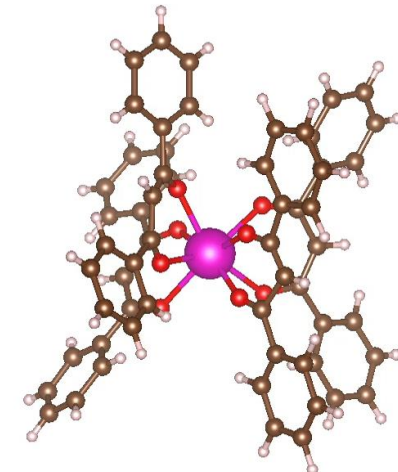
# PyFitIt Package: Machine Learning



- **PyFitIt**, a machine learning (*i.e.*, implementing **neural network**) based XANES simulation technique, exploiting the PyFitIt Python library with Python codes in Jupyter notebooks.
- **Direct** (prediction of a XANES spectrum for a given set of structural parameters) and **indirect** (prediction of a set of structural parameters for a given XANES spectrum) approaches for the XANES prediction and the corresponding 3D structural refinement.
- **FDMNES** or FEFF or ADF codes to calculate the *ab initio* theoretical XANES.
- **Euclidean ( $L_2$ ) norm**, integral of the squared difference between the theoretical & experimental XANES spectrum (like the Levenberg-Marquardt algorithm in Artemis Demeter, GNXAS etc., for EXAFS fit) .
- These methods developed for the Big Data or multidimensional data tasks and appropriate to run on the multicore's clusters (local computer very long time).
- 3D structure (XYZ) as input data and sampling points  $P_1, P_2, \dots, P_N$  for the training set can be selected by grid and improved Latin hypercube sampling (IHS).



Neural network implemented in PyFitIt



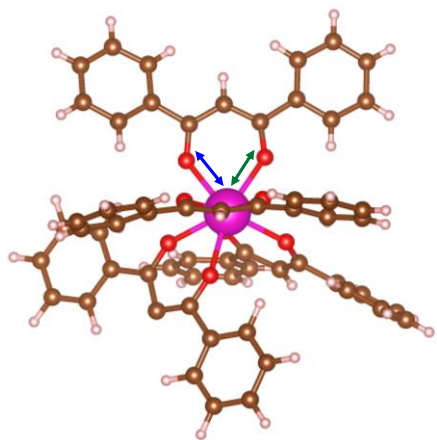
3D Structure



# PyFitIt XANES Simulation: $\text{Eu}^{3+}$ Tetrakis Complex



- PyFitIt, indirect approach to simulate the experimental XANES spectrum of  $\text{Eu}^{3+}$  tetrakis complex .
- FDMNES code to calculate the *ab initio* theoretical XANES.
- 3D structure (XYZ ) with experimental XANES were used as an input data.



5.2 Importing XANES calculated for training set

```
In [2]: sample = readSample('IHS_729')
```

5.3 Fitting XANES by sliders

```
In [8]: def addExtra(energy, intensity, params, context):
    sp = parseFdmnesFolder('fdmnes_ground0')
    smoothed, norm = smoothInterpNorm(smooth_params=context.getTransformParams('fdmnes_smooth'),
    spectrum=sp, smoothType='fdmnes',
    exp_spectrum=context.expSpectrum,
    fit_norm_interval=context.project.intervals['fit_norm'])
    context.plotData['ground'] = {'type': 'default', 'xData':smoothed.energy, 'yData':smoothed.intensity,
    'label':'ground', 'color':'red'}
    return energy, intensity

fitResult = fitBySliders(sample=sample, project=project,
    theoryProcessingPipeline=['approximation',
    'fdmnes_smooth', 'L2 norm', addExtra])
```

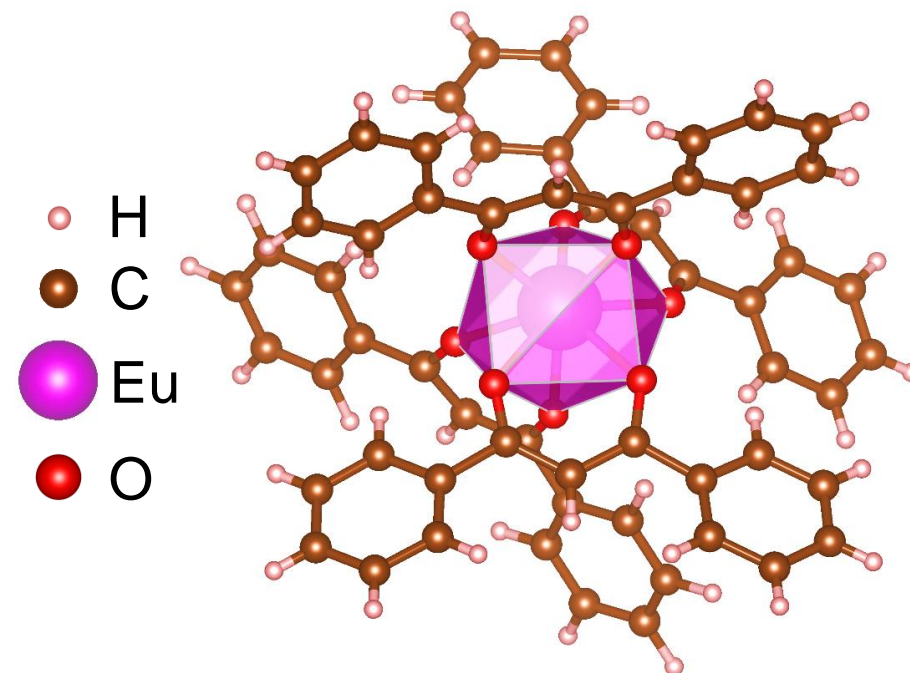
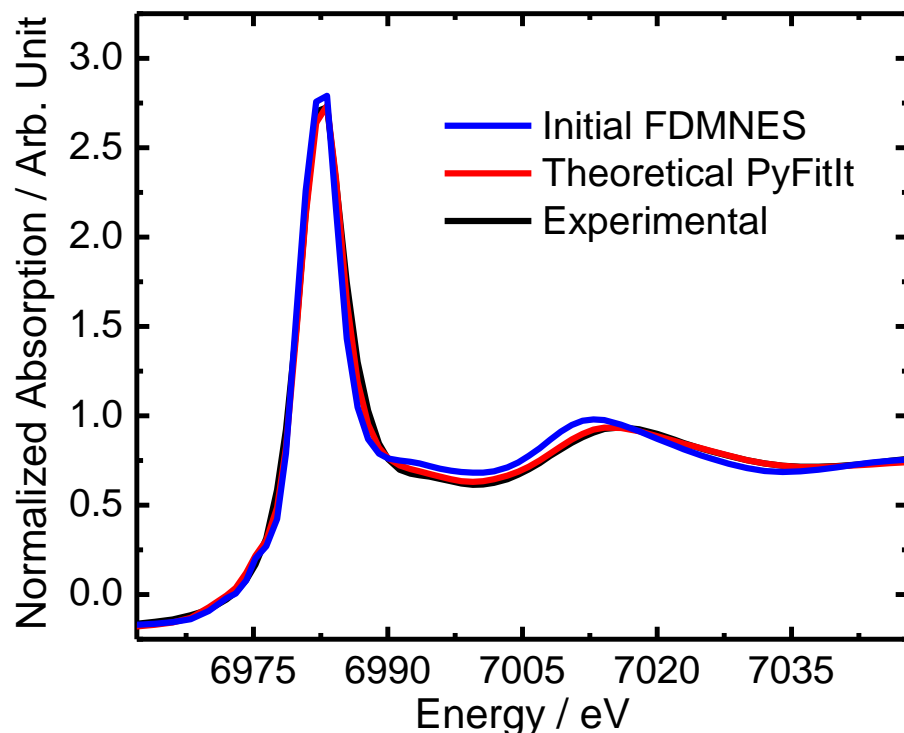
Figure 1

Legend: ground (red), theory (blue), experiment (black)

centralRing1_Shift	-0.17
centralRing2_Shift	-0.25
sideRings1_Elong	-0.12
sideRings1_Shift	0.12
sideRings2_Elong	0.18
sideRings2_Shift	0.04
Gamma_half	2.00

# PyFitIt XANES Simulation: Structure Refinement

- **Eu<sup>3+</sup> tetrakis  $\beta$ -diketonate complex [Eu(dbm)<sub>4</sub>(C<sub>4</sub>mim)]**  
dbm: dibenzoylmethane and C<sub>4</sub>mim: 1-butyl-3-methylimidazolium bromide



Experimental and theoretical XANES calculated at the Eu L<sub>3</sub>-edge using the FDMNES code directly and pyFitIt inverse method (left), and corresponding generated **distorted square antiprismatic structure** (right) for the Eu<sup>3+</sup> tetrakis complex [Eu(dbm)<sub>4</sub>(C<sub>4</sub>mim)].

# Applying Wavelet Transform - EXAFS Equation



## EXAFS Oscillation:

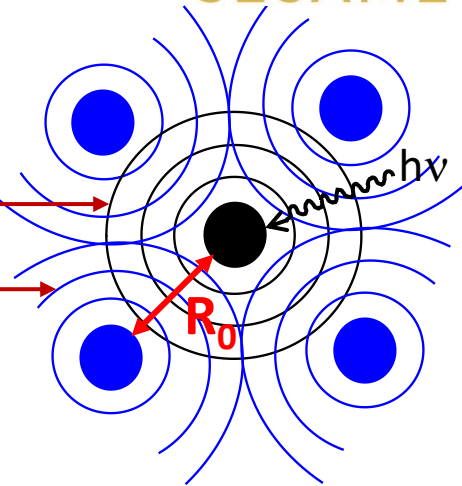
$\chi(k) = \sum_i \chi_i(k)$   $k$  is the photoelectron wavenumber

Each path can be written as:

$$\chi_i(k) = \left( \frac{(N_i S_0^2) F_i(k)}{k R_i^2} \sin(2kR_i + \varphi_i(k)) \exp(-2\sigma_i^2 k^2) \exp\left(-\frac{2R_i}{\lambda(k)}\right) \right)$$

Photo-electron wave

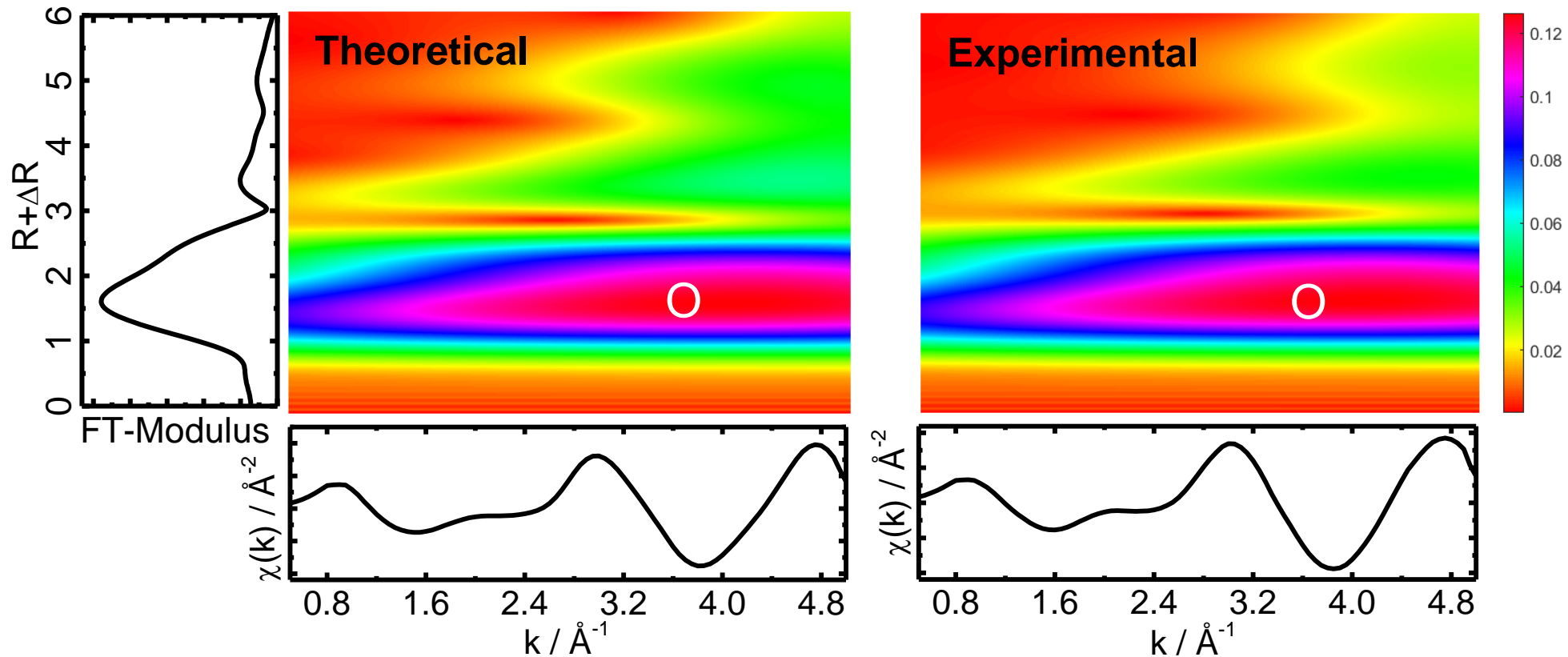
Back-scattered wave



- CCWT modulus visualizes the coordination shells of the neighboring atoms around the photoabsorber in form of RGB colored maps in the 2D and 3D CCWT images, simultaneously analyzing the input EXAFS data into respective two-dimensional  $k$  and  $R$  spaces.
- the lower atomic number atoms, such as O, more effectively backscatterers at lower  $k$  values, and high atomic numbers ones at higher  $k$  values, owing to the contribution of backscattering amplitude functions ( $F_i(k)$ ) of the neighboring atoms, associated with the number of repulsive electrons in their electronic clouds.



# Applying Wavelet Transform



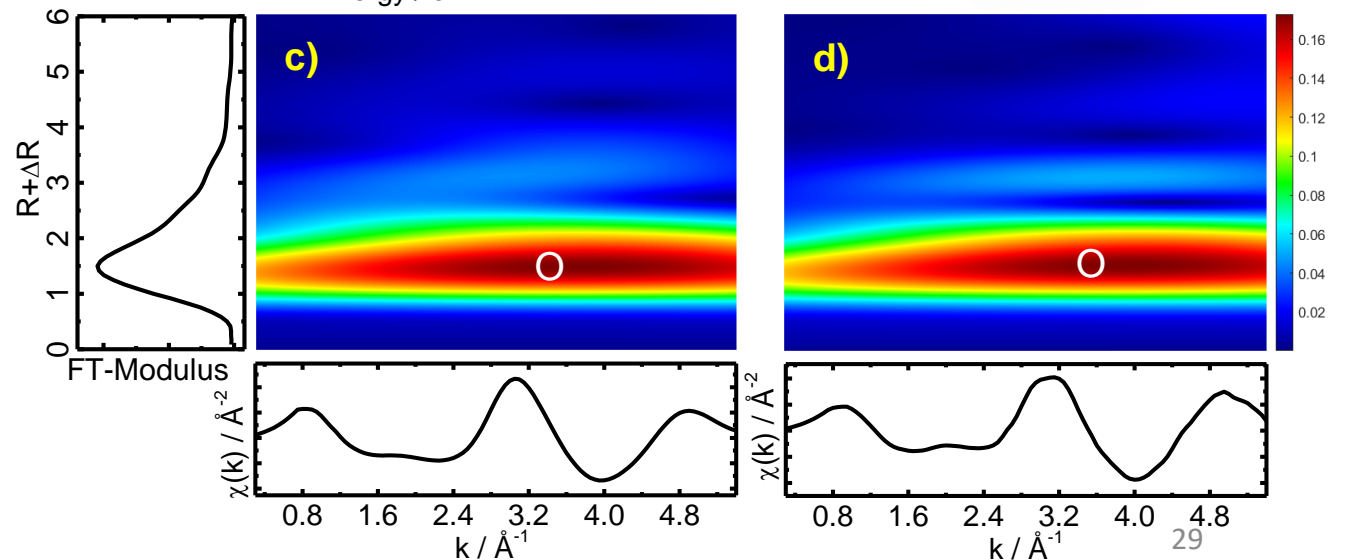
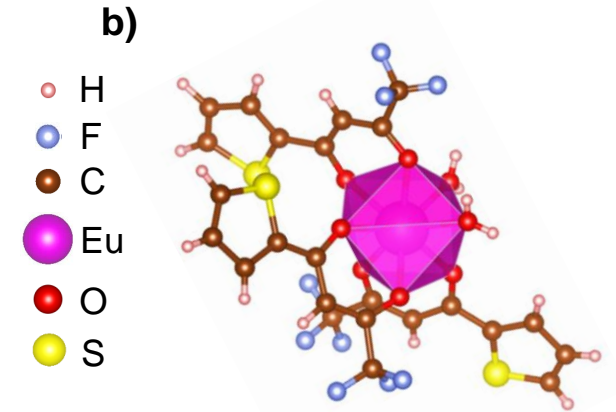
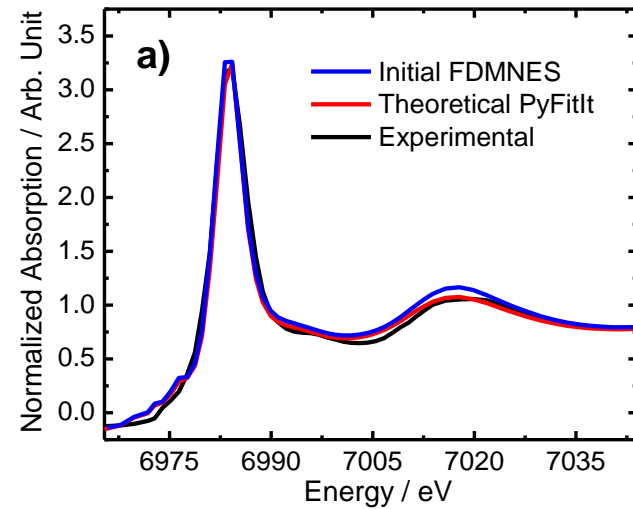
Continuous Cauchy wavelet transform analyses of theoretical (left) and experimental (right) XANES, showing the localization of O backscatterer as a pinkish red color map in similar pattern two-dimensional CCWT images.

# XANES Simulation: $\text{Eu}^{3+}$ *Tris* $\beta$ -Diketonate Complex

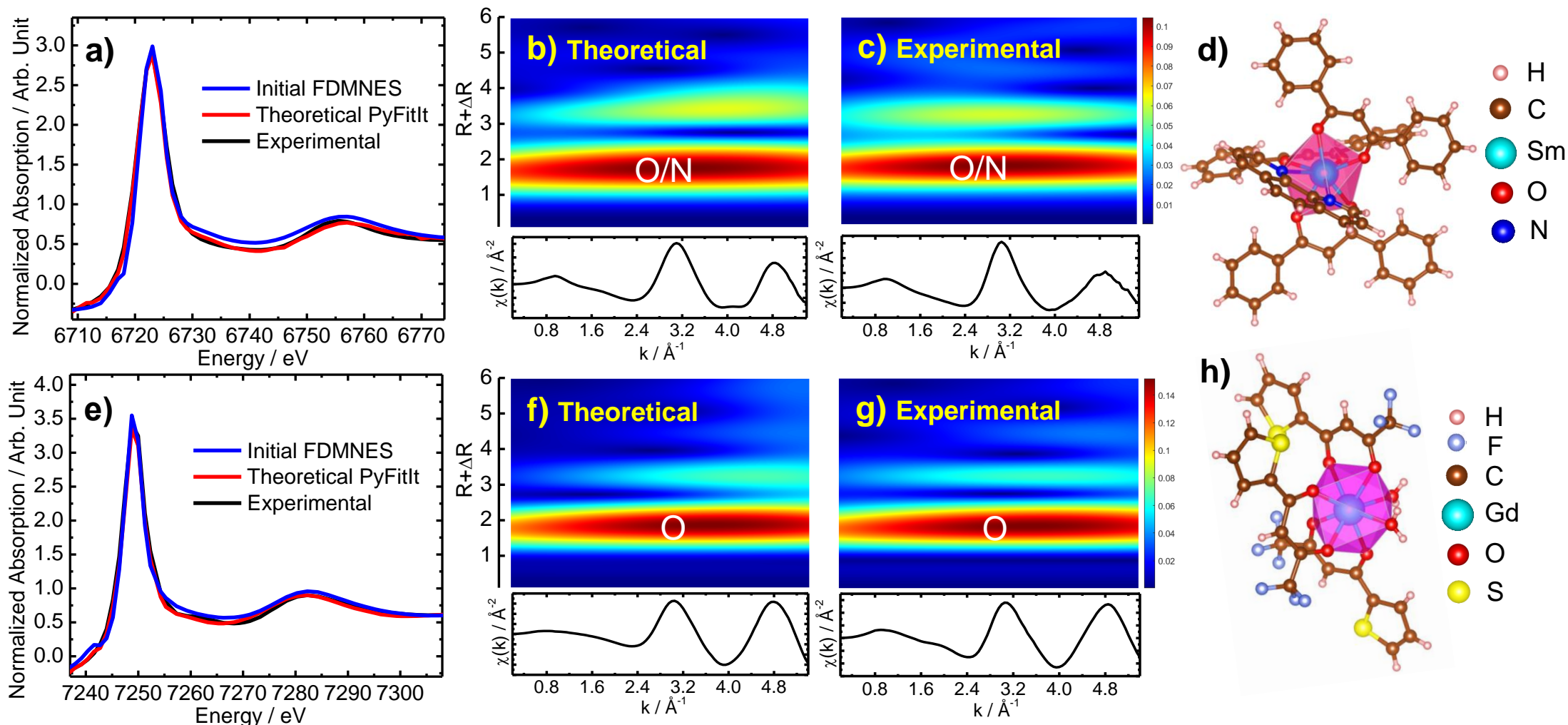
➤  $\text{Eu}^{3+}$  tris  $\beta$ -diketonate complex  $[\text{Eu}(\text{tta})_3(\text{H}_2\text{O})_2]$   
tta: 3-thenoyltrifluoroacetate

➤ Typical crystal structure

- Experimental and theoretical XANES calculated at the Eu  $L_3$ -edge using the PyFitIt inverse method (a)
- Corresponding square antiprismatic 3D structure for the  $[\text{Eu}(\text{tta})_3(\text{H}_2\text{O})_2]$  complex (b) .
- Continuous Cauchy wavelet transform analyses of theoretical (c) and experimental (d) XANES, showing the localization of O backscatterer as a dark-red color map in similar pattern two-dimensional CCWT images.



# XANES Simulation: $Gd^{3+}/Sm^{3+}$ $\beta$ -Diketonates



$Sm^{3+}$   $\beta$ -diketonate:  $[Sm(dbm)_3(phen)]$   
dbm: dibenzoylmethane, phen: phenanthroline

$Gd^{3+}$   $\beta$ -diketonate:  $[Gd(tta)_3(H_2O)_2]$   
tta: 3-thenoyltrifluoroacetate



# EXAFS Fit

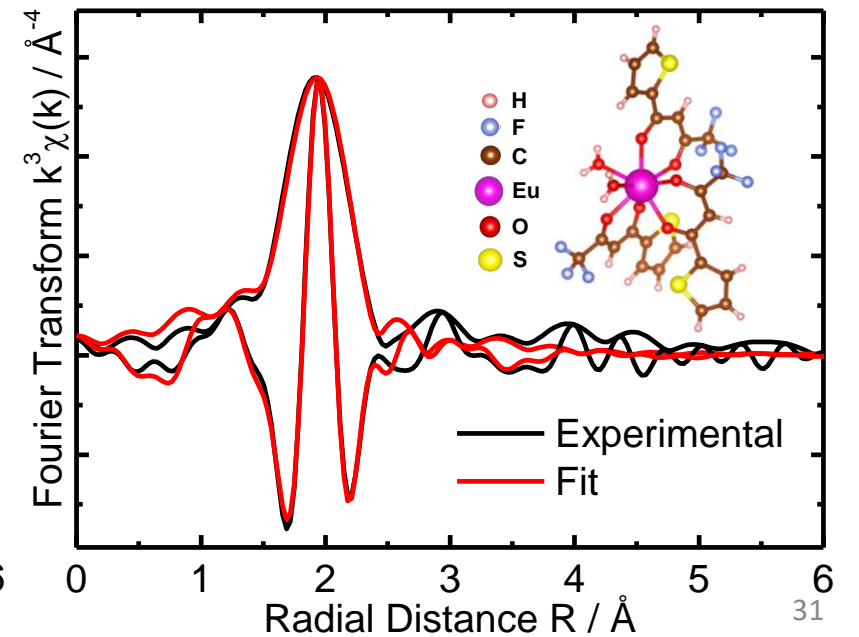
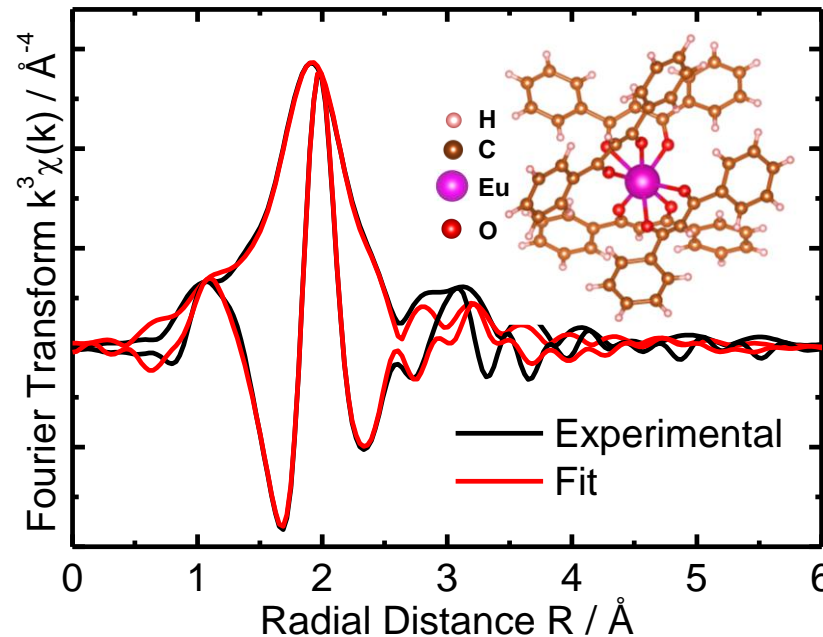
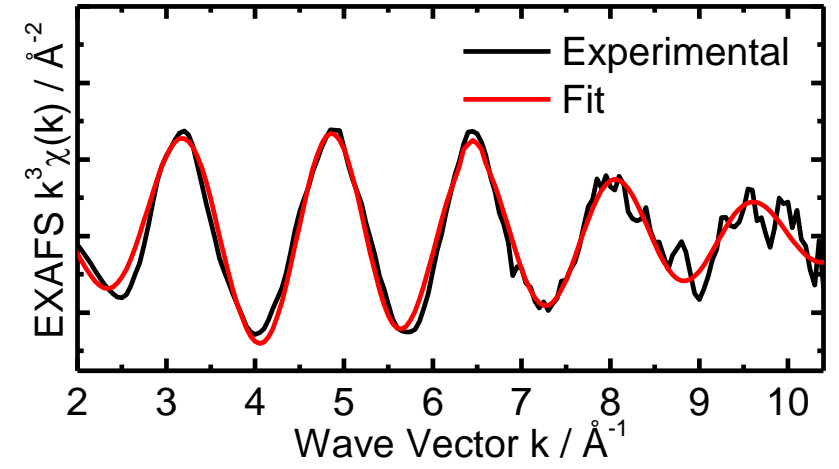
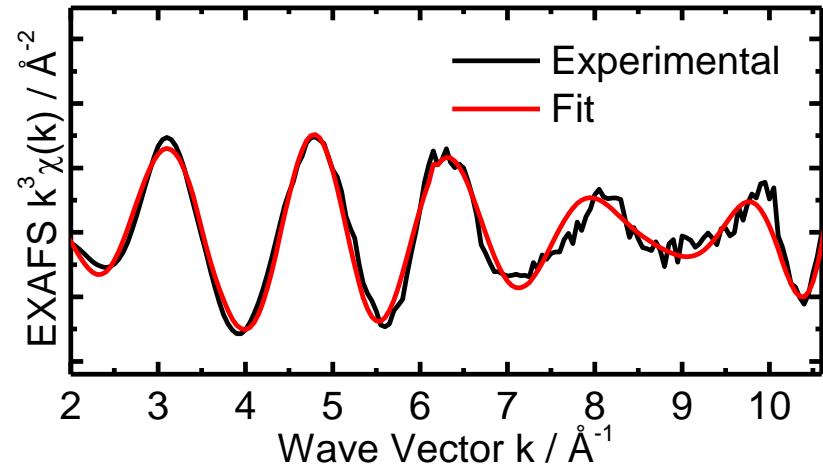
## ➤ EXAFS Fit: Artemis from Demeter

➤  $[\text{C}_4\text{mim}][\text{Eu}(\text{dbm})_4]$  complex (left)

➤  $[\text{Eu}(\text{tta})_3(\text{H}_2\text{O})_2]$  complex (right)

➤ The XYZ 3D structures obtained from the PyFitIt XANES simulation were used in EXAFS fit

➤ feff input files were generated from the corresponding 3D structures in MOLDRAW software



# EXAFS Fit



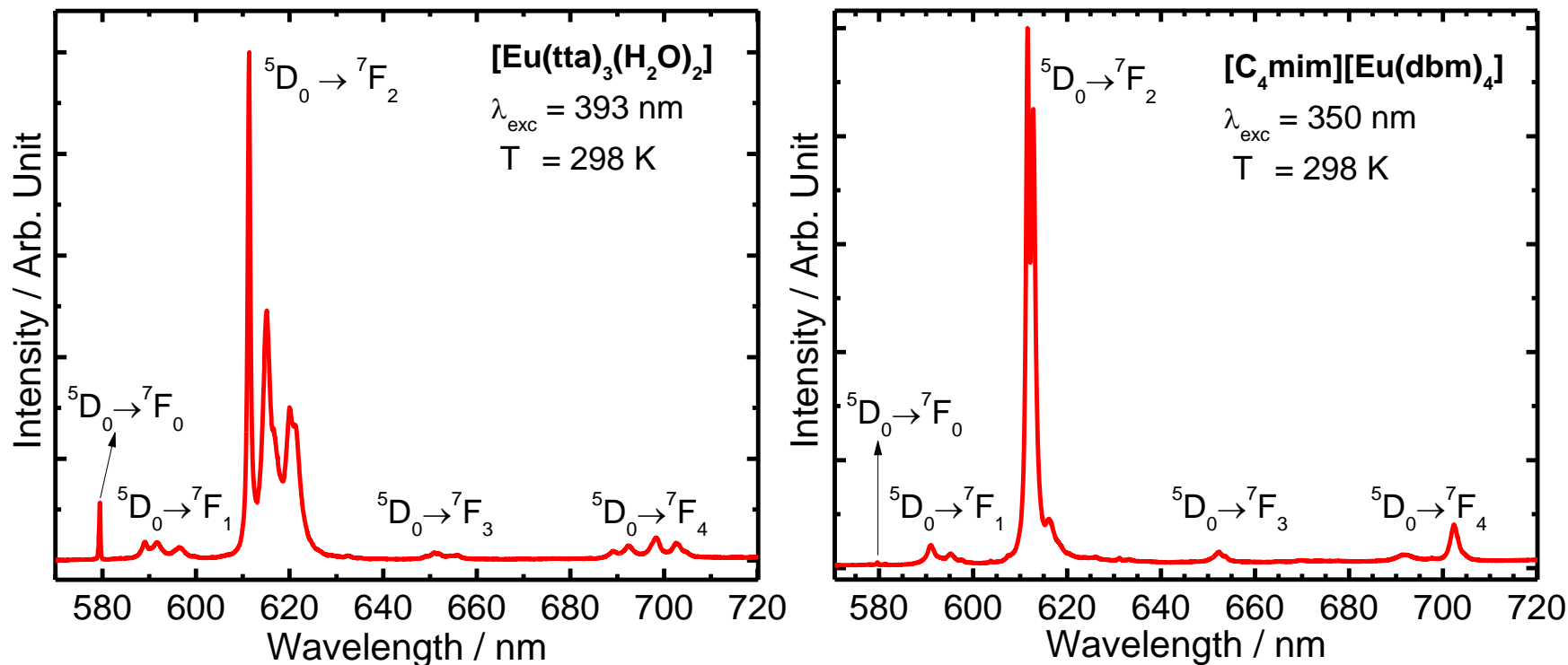
- **Artemis** employs FEFF8-lite code to calculate the values of the  $F_i(k)$  (effective scattering amplitude),  $\phi_i(k)$  (effective scattering phase shift) and  $\lambda$  (mean free path of the photoelectron).
- **IFEFFIT in Artemis** use Levenberg-Marquardt (algorithm) method of nonlinear least-squares minimization to minimize the standard  $\chi^2$  fitting metric:

$$\chi^2 = \frac{N_{idp}}{\varepsilon N_{data}} \sum_{i=\min}^{\max} \left[ \text{Re} \left( \chi_d(r_i) - \chi_t(r_i) \right)^2 + \text{Im} \left( \chi_d(r_i) - \chi_t(r_i) \right)^2 \right]$$

EXAFS fitting parameters:  $N_{\text{degen}}$ : degeneracy of the path,  $R$ : mean coordination shell radii,  $\sigma^2$ : mean square relative displacements (MSRDs) or Debye–Waller factor,  $S_0^2$ : passive electron reduction factor  $E_0$ : photoelectron energy and  $R_{\text{factor}}$ : goodness of the fit for the  $[\text{C}_4\text{mim}][\text{Eu}(\text{dbm})_4]$  and  $[\text{Eu}(\text{tta})_3(\text{H}_2\text{O})_2]$  complexes.

Complex	Bond	$N_{\text{degen}}$	$R(\text{\AA})$	$\sigma^2(\text{\AA}^2)$	$S_0^2$	$E_0$ (eV)	$R_{\text{factor}}$
<b><math>[\text{C}_4\text{mim}][\text{Eu}(\text{dbm})_4]</math></b>	Eu-O <sub>1</sub>	2	2.287±0.009	0.0105±0.0020	0.89	9.8	0.0074
	Eu-O <sub>2</sub>	3	2.434±0.007	0.0122±0.0021	0.89	9.8	0.0074
	Eu-O <sub>3</sub>	3	2.540±0.008	0.0091±0.0021	0.89	9.8	0.0074
<b><math>[\text{Eu}(\text{tta})_3(\text{H}_2\text{O})_2]</math></b>	Eu-O <sub>1</sub>	4	2.357±0.007	0.0058±0.0009	1.01	10	0.0040
	Eu-O <sub>2</sub>	2	2.436±0.007	0.0058±0.0009	1.01	10	0.0040
	Eu-O <sub>3</sub>	2	2.492±0.007	0.0077±0.0055	1.01	10	0.0040

# Validating PyFitIt XANES Simulation *via* Optical Properties



Emission spectra of the  $[\text{Eu}(\text{tta})_3(\text{H}_2\text{O})_2]$  (left) and  $[\text{C}_4\text{mim}][\text{Eu}(\text{tta})_4]$  (right) complexes recorded in solid state at 298 K temperature under excitations corresponded to the  $\text{S}_0 \rightarrow \text{S}_n$  transitions of the corresponding organic ligands.

Khan, L. U. et al. A Strategy to Probe the Local Atomic Structure of Luminescent Rare Earth Complexes by XANES Simulation Using Machine Learning Based PyFitIt Approach. *Inorganic Chemistry (ACS)*, 2023 (Accepted - In Press ).



# 4f-4f Intensity Parameters ( $\Omega_\lambda$ )

$$A_{0 \rightarrow J'}(\text{exp.}) = \frac{4e^2 \omega_{0 \rightarrow J'}}{3\hbar c^3 (2J+1)} \left[ \frac{n(n^2+2)^2}{9} \right] \left\langle {}^5D_0 \parallel U^{(\lambda)} \parallel {}^7F_\lambda \right\rangle^2 \Omega_\lambda(\text{exp.})$$

Refractive index

Lorentz local field correction ( $\chi$ )

Reduced element matrix

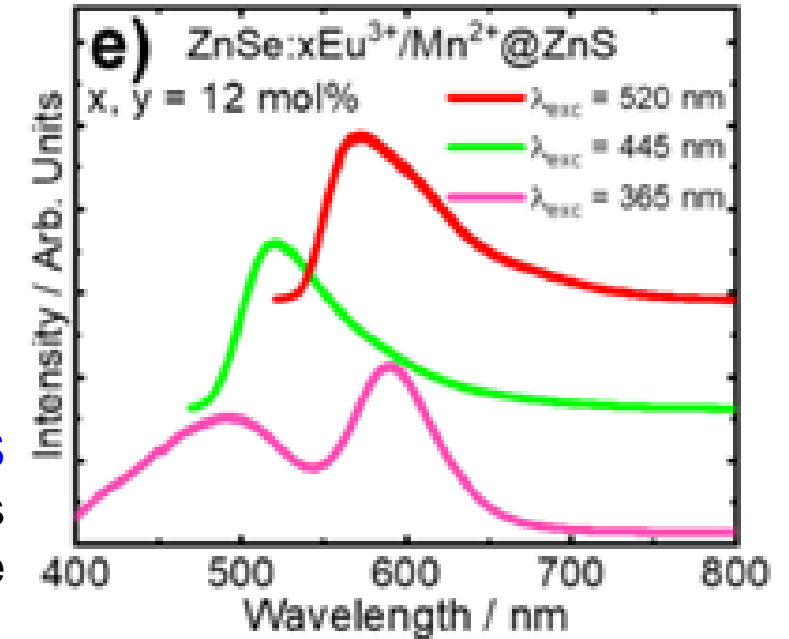
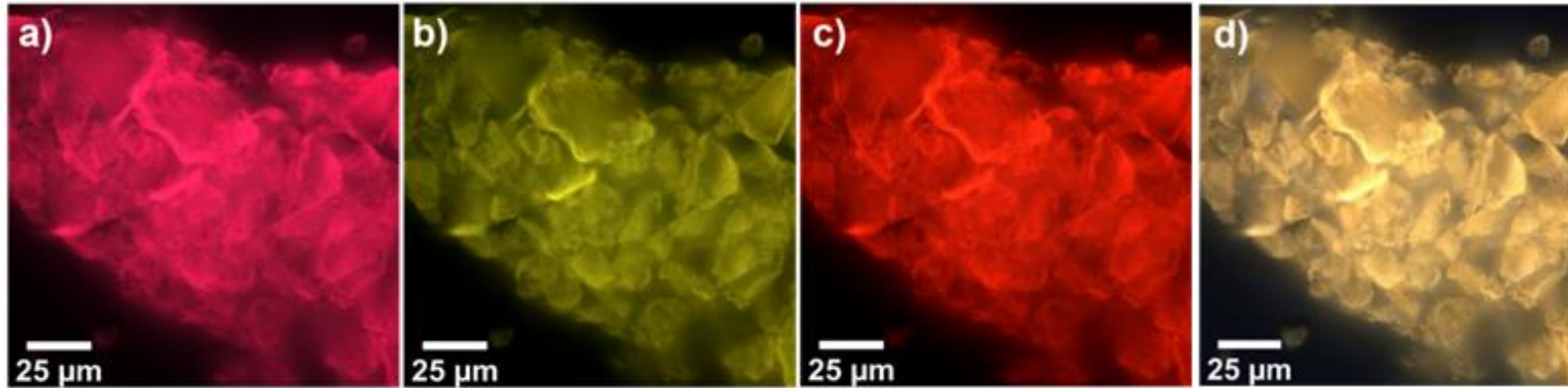
Experimental and theoretical intensity parameters ( $\Omega_\lambda$ ,  $\lambda = 2$  and  $4$ ) for the  $[\text{Eu}(\text{tta})_3(\text{H}_2\text{O})_2]$  and  $[\text{C}_4\text{mim}][\text{Eu}(\text{tta})_4]$  complexes.

Complex	$\Omega_2$		$\Omega_4$	
	Experimental	PyFitIt	Experimental	PyFitIt
$[\text{C}_4\text{mim}][\text{Eu}(\text{dbm})_4]$	$29 \pm 1$	$28.99 \pm 0.08$	$5.8 \pm 0.7$	$5.80 \pm 0.14$
$[\text{Eu}(\text{tta})_3(\text{H}_2\text{O})_2]$	$32 \pm 1$	$32.00 \pm 0.01$	$6.8 \pm 0.8$	$7.07 \pm 0.01$

The spontaneous emission coefficients ( $A_{0 \rightarrow J}$ ) are given by

$$A_{0 \rightarrow J} = \left( \frac{S_{0 \rightarrow J}}{S_{0 \rightarrow 1}} \right) A_{0 \rightarrow 1}$$

# Wide Visible-Range Fluorescence QDs



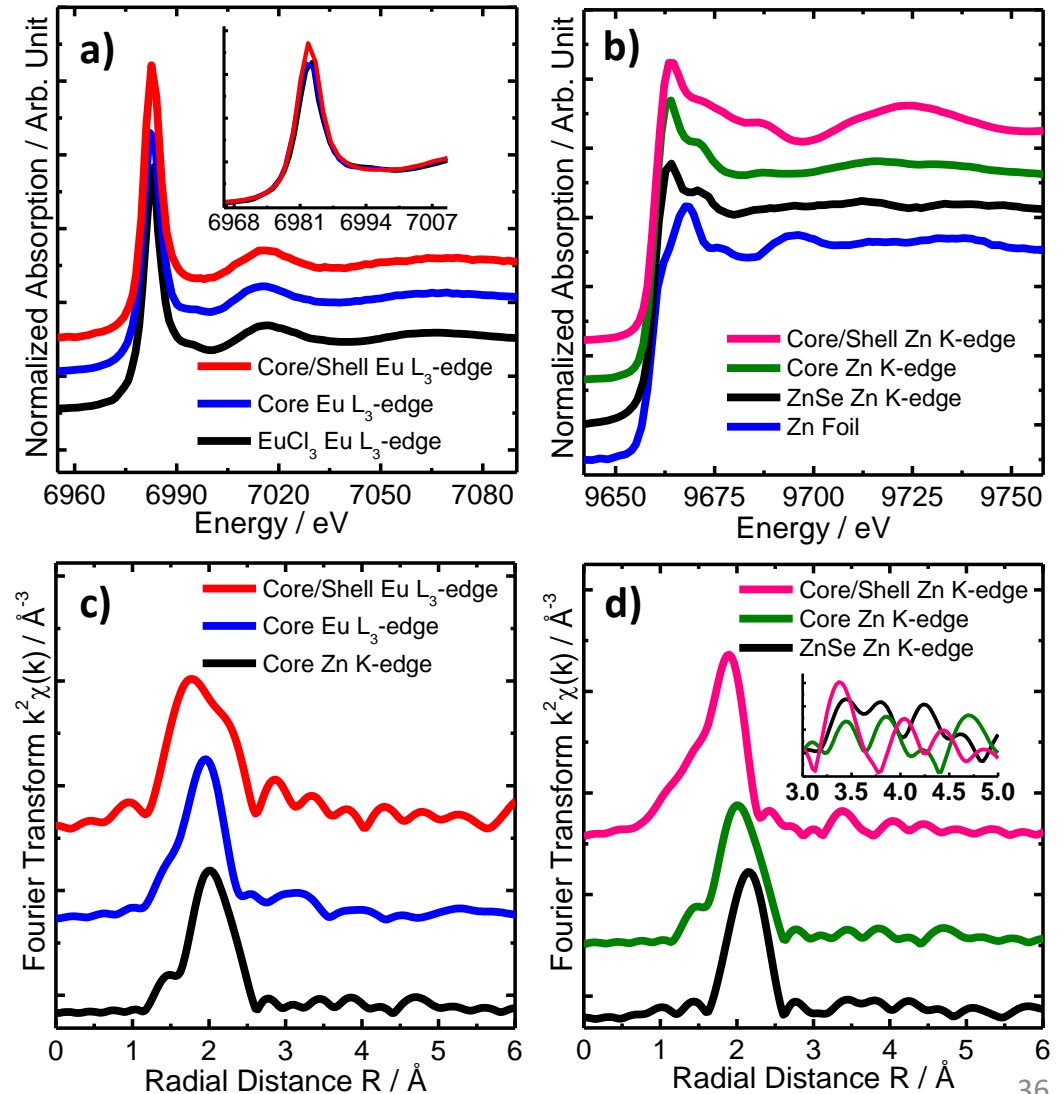
CytoViva dual-mode fluorescence images of aqueous ZnSe:Eu<sup>3+</sup>,Mn<sup>2+</sup>@ZnS core/shell QDs dispersion, measured at different excitation wavelengths ( $\lambda_{exc}$ ): 390 nm (a), 445 nm (b), 520 nm (c), white light (d), and the corresponding emission spectrum (e).

- **Unraveling the excitation wavelength dependent tunable emission color:**
  - Energy transfer mechanism among metal ions dopants and host lattice.
  - X-ray absorption spectroscopy (XAFS) to probe metals local structure and oxidation states with optical properties needed.
  - XEOL in combination with XANES may ideal.

# Probing Local Structure of QDs by XAFS

Normalized XANES spectra (a,b) and the Fourier transforms of their  $k^2$ -weighted EXAFS [ $\chi(k)$ ] (c,d) for the ZnSe:Eu<sup>3+</sup>,Mn<sup>2+</sup> core and ZnSe:Eu<sup>3+</sup>,Mn<sup>2+</sup>@ZnS core/shell QDs collected at the Eu L<sub>3</sub>-edge (6977 eV) and Zn K-edge (9659 eV).

- K-edge of Zn in sulfides exhibited three well-defined peaks till 50 eV above the edge, and only two peaks in selenides, because the  $p$ -like densities of states mainly determined by the type of counter anion, Se and S in ZnSe and ZnS lattice, respectively.
- Eu<sup>3+</sup> ion occupy sites in both ZnSe and ZnS cubic lattice.



# Optical Properties of QDs

UV-visible absorption spectra (a), excitation spectra (b) and emission spectra (c) of ZnS passivated ZnSe:Eu<sup>3+</sup>,Mn<sup>2+</sup> and ZnSe:Eu<sup>3+</sup> core/shell QDs, and schematic representation of energy level diagram (d).

**Publication:** Zahid U Khan, Mayara K Uchiyama, Latif U Khan et al. *Journal of Materials Chemistry B* (RSC) 2022.

DOI: <https://doi.org/10.1039/D1TB01870A>

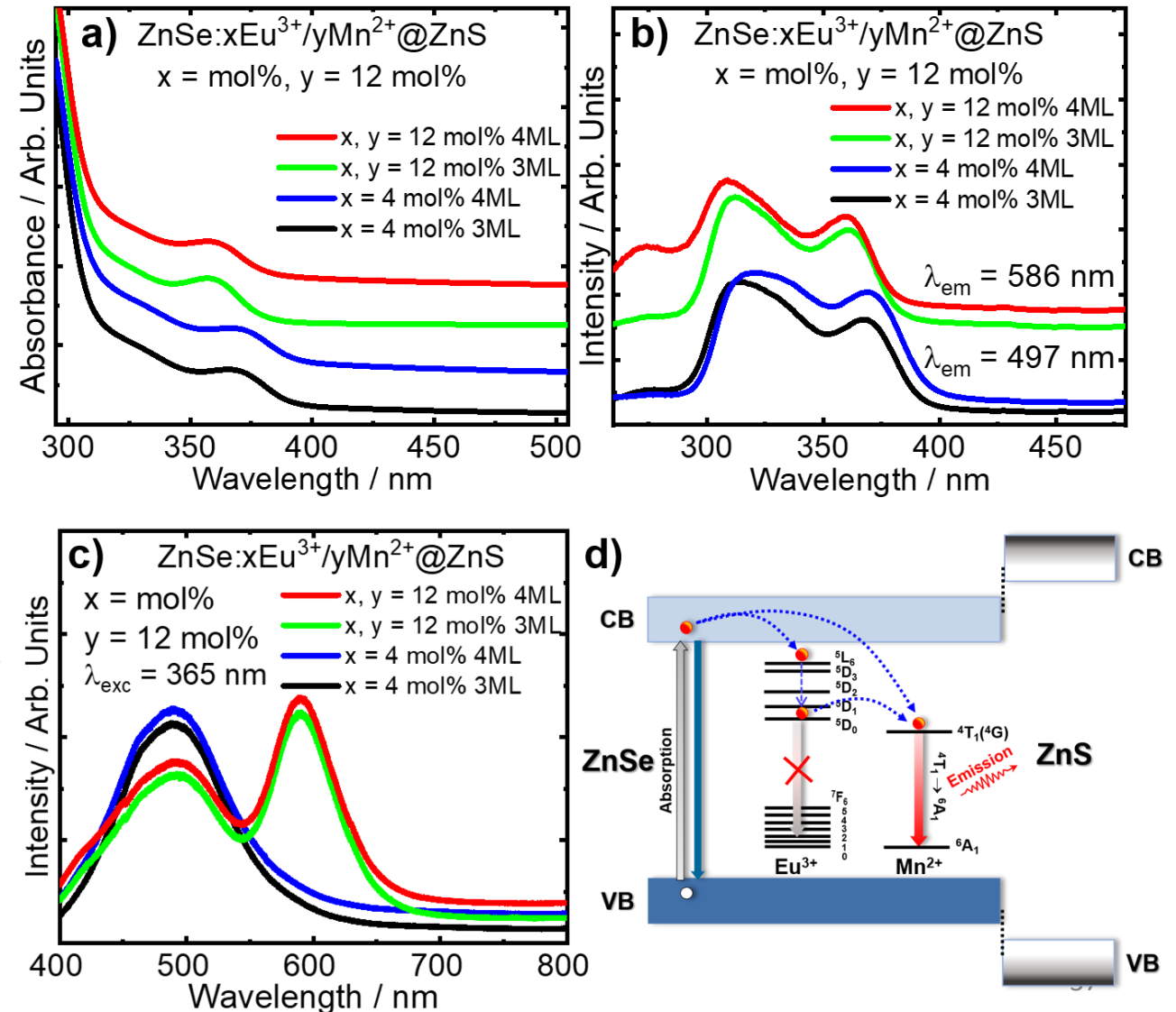


From the journal:  
**Journal of Materials Chemistry B**

**Wide Visible-Range Activatable Fluorescence ZnSe:Eu<sup>3+</sup>/Mn<sup>2+</sup>@ZnS Quantum Dots: Local Atomic Structure Order and Application as a Nanoprobe for Bioimaging**



Zahid Ullah Khan, Mayara Klimuk Uchiyama, Latif Ullah Khan, Koiti Araki, Hiro Goto, Maria Cláudia F.C. Felinto, Ana Olívia de Souza, Hermi Felinto Brito and Magnus Gidlund

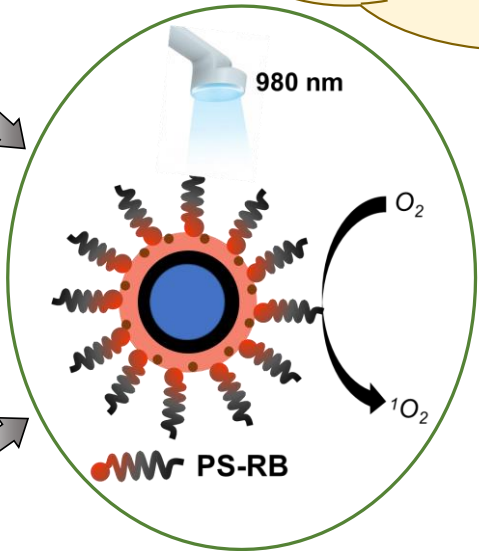
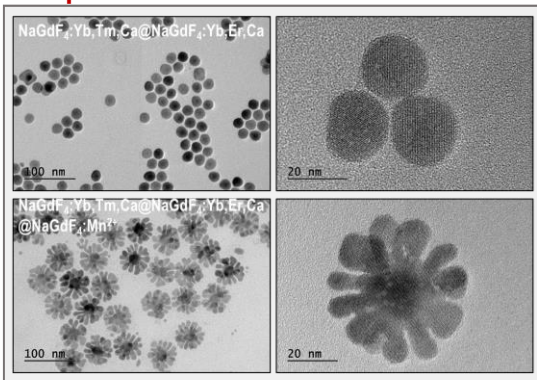
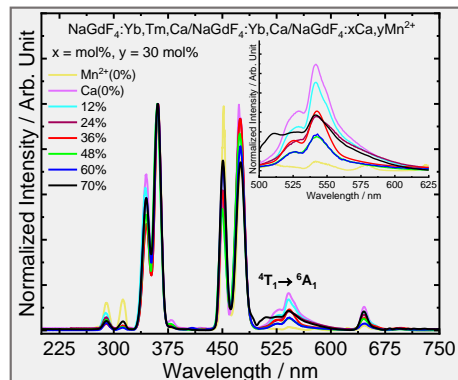




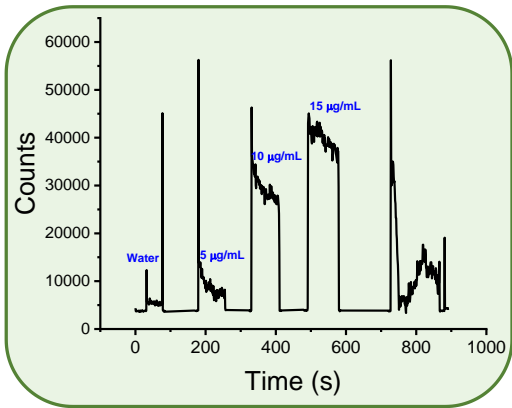
# Singlet Oxygen ( $^1O_2$ ) Generation: Luminescence NPs as Amplifiers/Sensitizers



Upconversion Nanoparticles



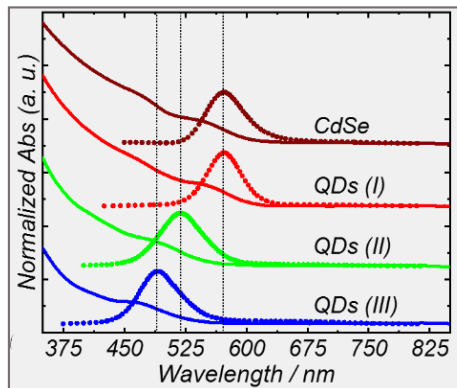
XANES in combination with UC/DC-Luminescence/XEOL can provide deep insight on local electronic structure and energy levels structure of metals ions to probe the energy transfer and luminescence mechanism in nanophosphors, acting as amplifiers for singlet oxygen ( $^1O_2$ ) generation.



The spherical and flowers shapes visible luminescence nanophosphors act as efficient amplifiers for singlet oxygen ( $^1O_2$ ) generation, under irradiation with UV-vis and near-IR (980 nm) laser.



Quantum Dots (QDs)



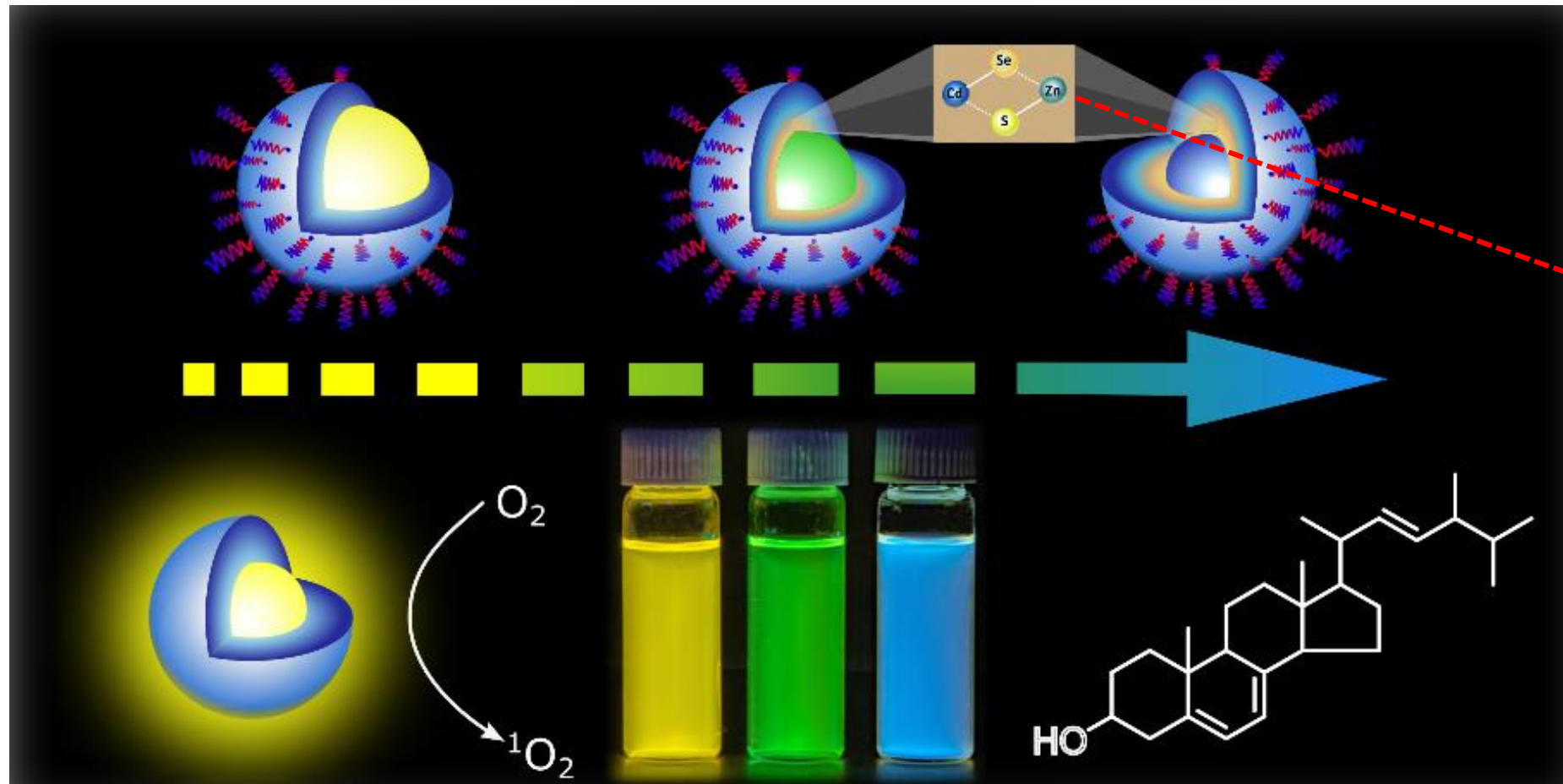
# Emission Color-Tunable CdSe/ZnS QDs as Photosensitizers for $^1\text{O}_2$ Generation



Yellow - QDs (I)

Green - QDs (II)

Blue - QDs (III)



**Anion exchange  
at interface  
alloying**

# Probing Anion Exchange in Core/Shell QDs by XAFS

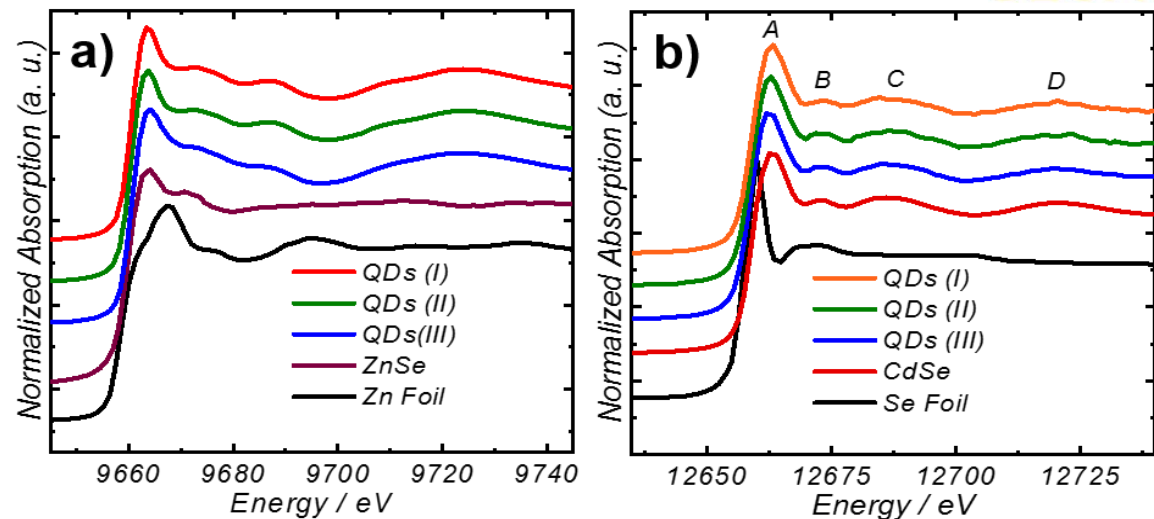
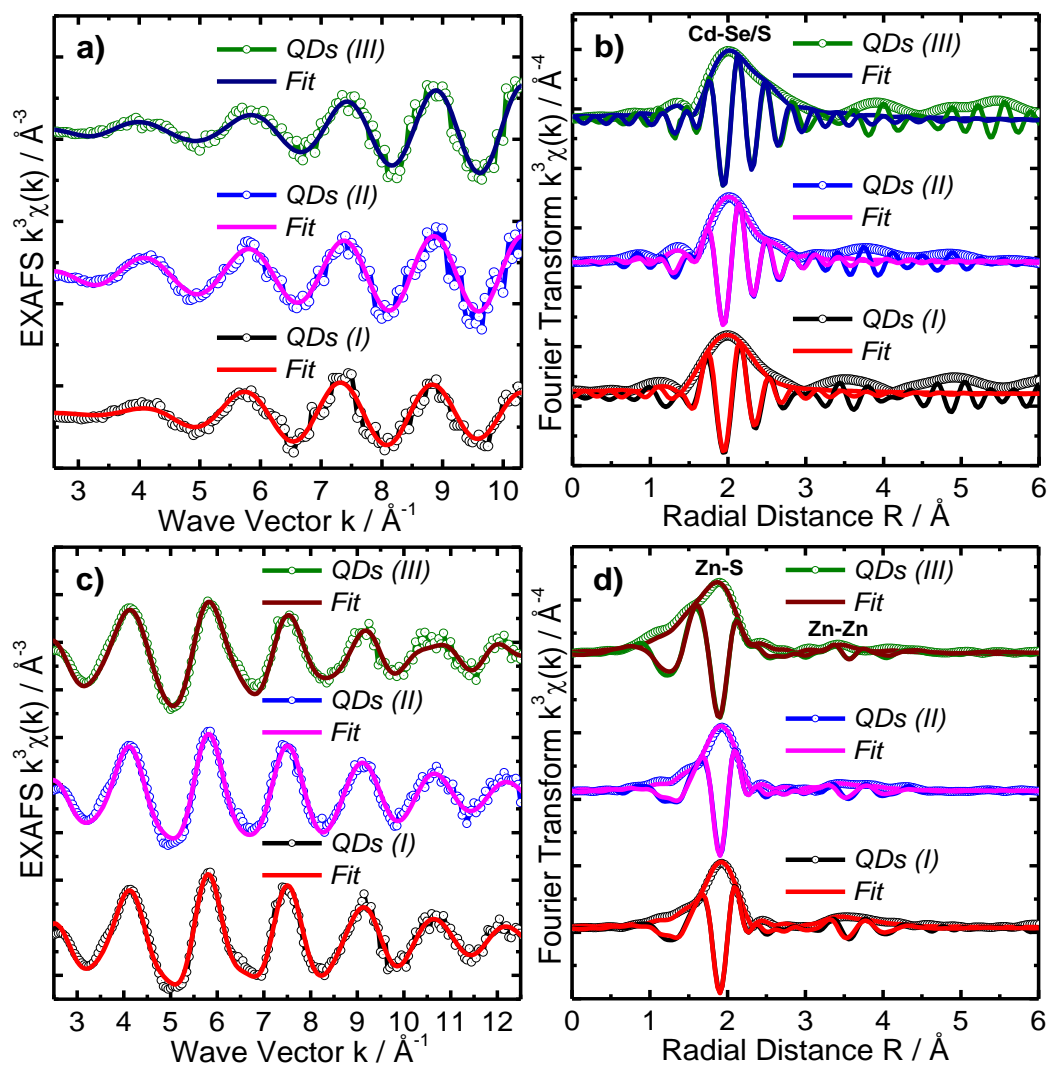


**Table 1.** Derived EXAFS fitting parameters, including N: number of neighboring atoms, R: distance between absorbing atom and its neighbors,  $\sigma^2$ : mean square relative displacements (MSRDs) or Debye–Waller factor,  $S_0^2$ : amplitude reduction factor and  $R_{factor}$ : goodness of fit for the QDs (I), QDs (II), and QDs (III).

Material	Bond Type	N	R( $\text{\AA}$ )	$\sigma^2(\text{\AA}^2)$	$S_0^2$	$R_{factor}$
QDs (I)	Cd-Se	4	2.531±0.008	0.01048±0.00088	1.0	0.0310
QDs (III)	Cd-S	2	2.494±0.009	0.00189±0.00055	0.9	0.0092
	Cd-Se	2	2.567±0.009	0.01368±0.00710	0.9	0.0092
QDs (III)	Cd-S	2.7	2.516±0.005	0.00929±0.00334	0.7	0.0211
	Cd-Se	1.3	2.589±0.005	0.00160±0.00092	0.7	0.0211



# Energy Conversion and Storage Devices - Renewable Energy



- Nickel ion-implanted Cobalt (II) Oxides thin films deposited on the Fluorine-doped Tin Oxide (FTO) glass (Fixed fluence:  $1 \times 10^{15} \text{ cm}^{-2}$ ), using Pelletron Tandem Accelerator (Energy: 700 KeV).



**Energy:** 700 keV-35 MeV  
**Beam spot:** 0.5 to 8 mm

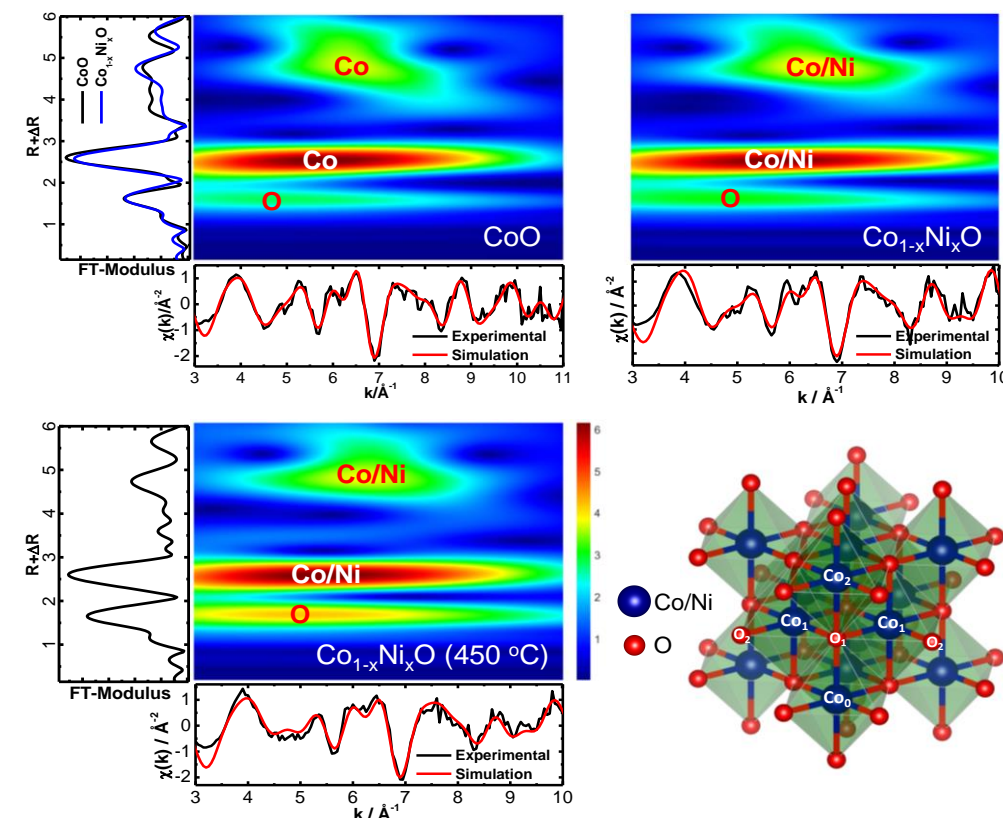
**Ion beams :** H, He, B, P, C, Si, P, Ni, Cu, Fe, Au

- Exploring defects/oxygen vacancies in these samples *via* XAFS to enhance their efficiencies for application as electrocatalysts in Hydrogen Evolution Reaction - HER (Fuel Cells).

**Dr. Naila Jabeen Rresearch Group from National Center of Physics Pakistan**

**Publication:** Sadaf Jamil, Naila Jabeen, Latif Ullah Khan, et al. Synthesis and Comparative Evaluation of Optical and Electrochemical Properties of Efficacious Heterostructured-Nanocatalysts of ZnSe with Commercial and Reduced Titania. *Journal of Alloys and Compounds (Elsevier)*, 879, 160449, 2021. DOI: <https://doi.org/10.1016/j.jallcom.2021.160449>

EXAFS Simulation by Evolutionary Algorithm Implemented in Reverse Monte Carlo method (EA-RMC).



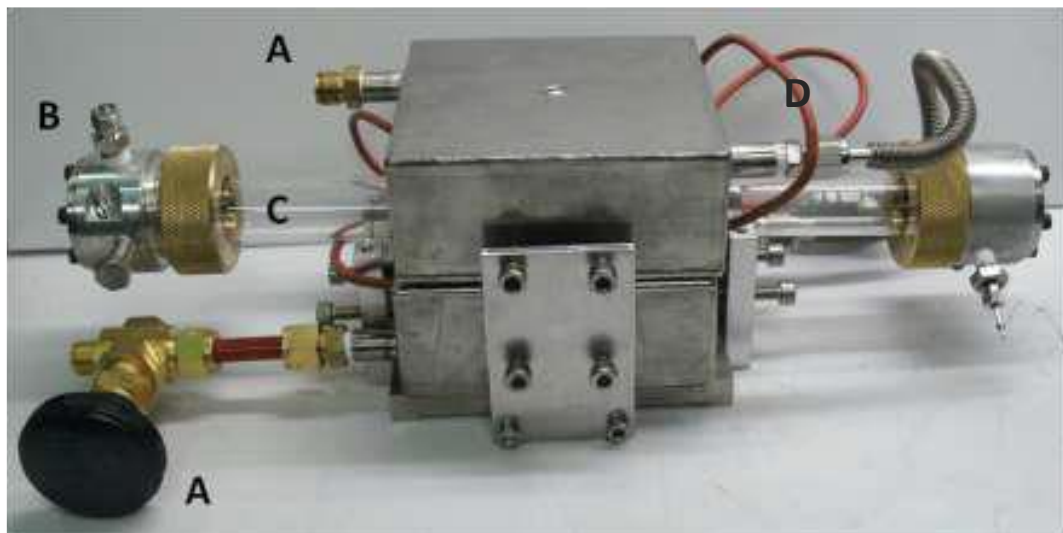
**Publication:** Latif Ullah Khan, Naila Jabeen et al. Investigating Local Structure of Ion-Implanted ( $\text{Ni}^{2+}$ ) and Thermally Annealed Rocksalt CoO film by EXAFS Simulation Using Evolutionary Algorithm. *ACS Applied Energy Materials (ACS)* 4, 2049–2055, 2021. DOI: <https://doi.org/10.1021/acs.aem.0c02676>



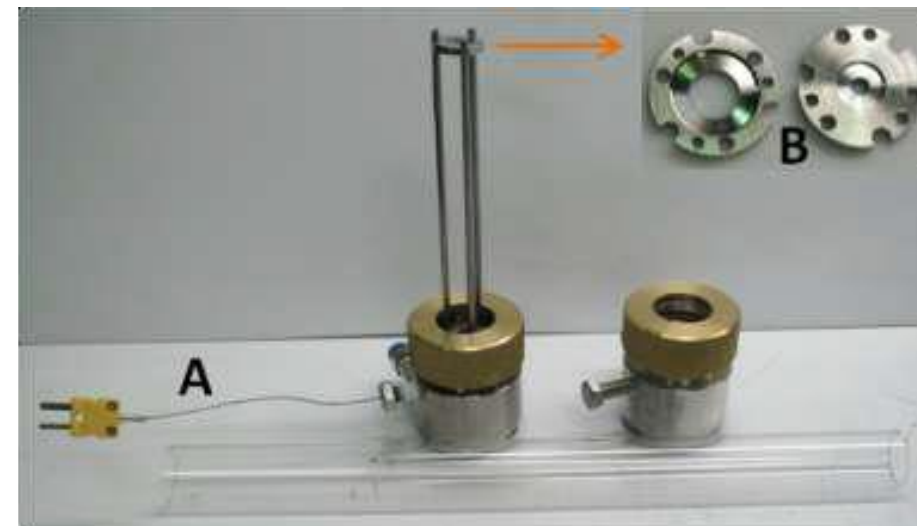
# Sample Environment - Tubular Furnace/Reactor

- Tubular Furnace/Reactor: A Sample Environment for In-Operando X-ray Absorption Studies (Catalysis)

Temperature (°C)	Sample Holder Ø mm	Atmospheres	Controller
Up to 800	8	Gases, Vapors and Vacuum	Programmable Logic Controller (PLC), SEASME



A: Inlet and outlet for water cooling  
B: Inlet and outlet for gases with Kapton windows  
C: Quartz glass tube

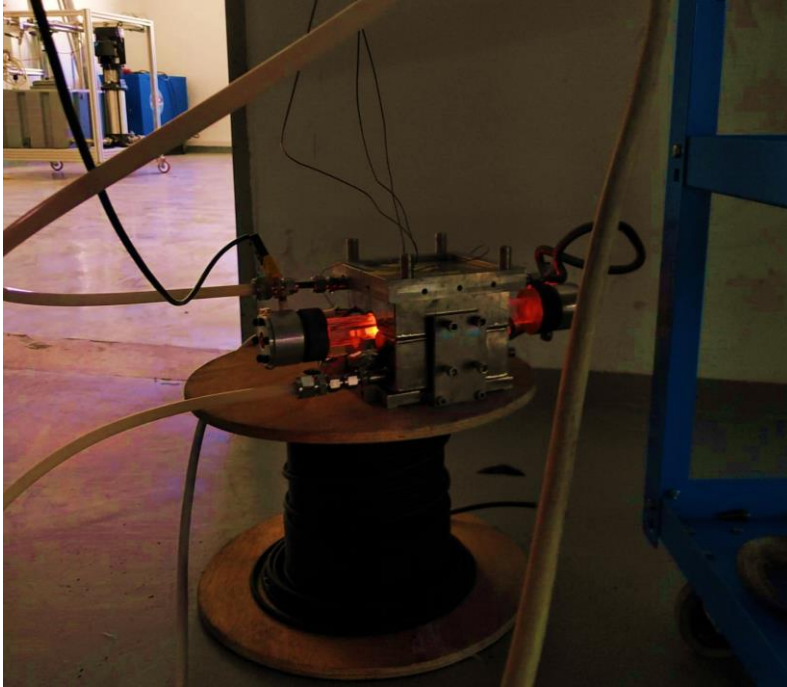


A: Thermocouple on the sample  
B: End sample holder

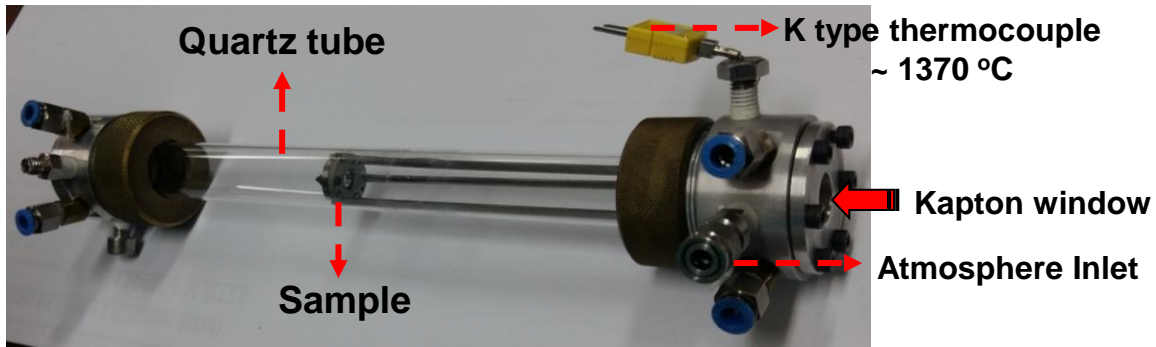
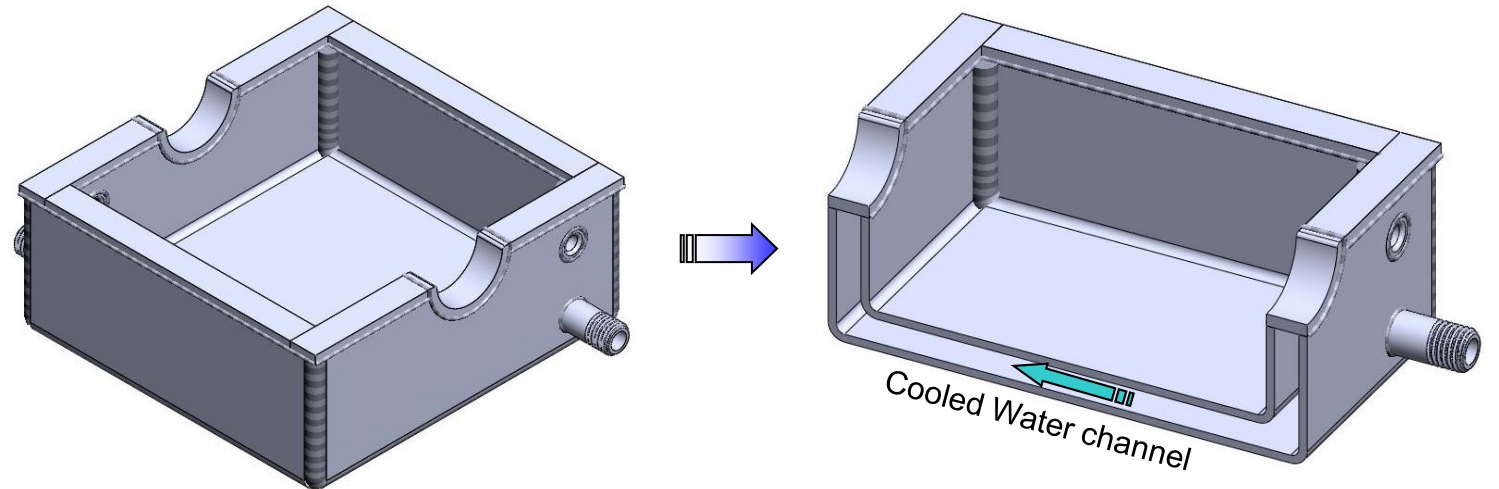
Collaboration: Dr. Santiago J. A. Figueroa QUATI Beamline

# Sample Environment For Catalysis

## ❑ In-House Preparation of Tubular Furnace



## ❑ Main steel chamber *In-house* design



- Highly stable temperature response (400-800 °C)
- Efficient cooling
- Two models: i) 25-400 °C and ii) 400-800 °C range
- Installation of thermal and water flow switches

# Publications (2022-2023)



- 1) Harfouche, M. et al. Emergence of the first XAFS/XRF beamline in the Middle East: providing studies of elements and their atomic/electronic structure in pluridisciplinary research fields. *J. Synchrotron Rad.*, 29, 1-7, 2022.

## Nanophosphors

- 1) Rehman, A.U.; Khan, L.U.; Brito, H.F.; Khan, Z.U. and Khan, A.M. Surfactant-based synthesis of optically active colloidal  $\text{GdF}_3:\text{Ce}^{3+}(5\%)\text{Eu}^{3+}(\chi\%)$  and  $\text{GdF}_3:\text{Ce}^{3+}(5\%)\text{Eu}^{3+}(5\%)/\text{SiO}_2$  phosphor nanocomposites. *Applied Nanoscience (Springer)*, 12, 2183–2193, 2022.
- 2) Khan, Z.U.; Uchiyama, M.K.; Khan, L.U.; Araki, K.; Goto, H.; Felinto, M.C.F.C.; De Souza, A.O.; Brito, H.F.; Gidlund, M. Wide Visible-Range Activatable Fluorescence  $\text{ZnSe}:\text{Eu}^{3+}/\text{Mn}^{2+}@\text{ZnS}$  Quantum Dots: Local Atomic Structure Order and Application as a Nanoprobe for Bioimaging. *J. Mater. Chem. B (RSC)*, 10, 247-261, 2022.
- 3) Khan, L.U.; Khan, Z.U.; Blois, L.; Tabassam, L.; Brito, H.F. and Figueroa, S.J.A. A New Strategy to Probe the Local Atomic Structure of Luminescent Rare Earth Complexes by XANES Simulation Using Machine Learning Based PyFitIt Approach. *Inorganic Chemistry (ACS)*, 2023 (Accepted InPress).
- 4) Khan, Z.U.; Khan, L.U. et al. Singlet Molecular Oxygen Generation via Unexpected Emission Color-Tunable  $\text{CdSe}/\text{ZnS}$  Nanocrystals. *ACS Applied Nano Materials (ACS)*, 2023 (In Revision).

## Catalysis

- 1) Sajid, F.; Jabeen, N.; Khan, L.U. et al. Local atomic structure order and electrochemical properties of NiO based nano-catalysts for ethanol sensing at room temperature. *Journal of Physics and Chemistry of Solids (Elsevier)*, 175, 111201, 2023.
- 2) Qadeer, N.; Jabeen, N.; Khan, L.U.; Sohail, M.; Zaheer, M.; Vaqas, M.; Kanwal, A.; Sajid, F.; Qamar, S. and Akhter, Z. Hydrothermal Synthesis and Characterization of Transition Metal (Mn/Fe/Cu) Co-Doped Cerium Oxide-Based Nano-Additives for Potential Use in the Reduction of Exhaust Emission from Spark Ignition Engines. *RSC Adv. (RSC)*, 12, 15564-15574, 2022.
- 3) Rubab, A.; Baig, N.; Sher, M.; Ali, M.; Ul-Hamid, A.; Jabeen, N.; Khan, L.U.; Sohail, M. Synthesis and Characterization of a Carbon-Supported Cobalt Nitride Nano-Catalyst. *ChemNanoMat. (Wiley Online Library)* e202100428, 2022.
- 4) Jamil, S.; Jabeen, N.; Khan, L.U.; Akhter, Z. et al. Synthesis and Comparative Evaluation of Optical and Electrochemical Properties of Efficacious Heterostructured-Nanocatalysts of ZnSe with Commercial and Reduced Titania. *Journal of Alloys and Compounds (Elsevier)*, 879, 160449, 2021.
- 5) Khan, L.U.; Jabeen, N.; et al. Investigating Local Structure of Ion-Implanted ( $\text{Ni}^{2+}$ ) and Thermally Annealed Rocksalt CoO film by EXAFS Simulation Using Evolutionary Algorithm. *ACS Appl. Energy Mater. (ACS)*, 4, 2049–2055, 2021.



# Acknowledgments



Dr. Carlos Pérez  
XRF - Carnauba BL  
(SIRIUS LNLS)



Prof. Hermi F Brito  
Electr. Spectroscopy  
(IQ-USP)



Prof. Oscar Malta  
Theor. Electr. Spectroscopy  
(DQF-UFPE)



Prof. Marcelo Knobel  
Nanomagnetism Physics IFGW  
(Rector -UNICAMP)



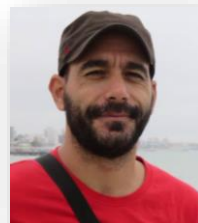
Dr. Diego Martinez  
Nanotechnology  
(LNNano-CNPEN)



Dr. Santiago Figueroa  
XAFS - QUATI BL  
(SIRIUS LNLS)



Dr. Messaoud Harfouche  
XAFS/XRF BL  
(SESAME)



Prof. Diego Muraca  
Nanomagnetism/Microscopy  
(IFGW-UNICAMP)



Prof. Kleber  
Magnetism Physics  
(IFGW-UNICAMP)



Dr. Maria C.F.C. Felinto  
Rare Earths (IPEN)



Dr. Vronica Teixeira  
XEOL - Carnauba BL  
(SIRIUS LNLS)



Dr. Muhammad Usman  
Ion Beam Accelerator  
(NCP Islamabad)



Dr. Naila Jabeen  
Catalysis Nanotechnology  
(NCP Islamabad)



Prof. Magnus  
Immune Physiopathology  
(ICB-USP)



Dr. Zahid Khan  
Nanobiotechnology  
(ICB-USP)



# Thanks

---



# Thanks

Thanks